UNIVERSITY OF TARTU
Faculty of Science and Technology Institute of Technology

Oyedele OLAOYE

Investigation of Dopamine-mediated Toxicity in Parkinsonian Sensory Neurons

Master's Thesis (30 ECTS) Curriculum Bioengineering

Supervisor: Miriam A. Hickey PhD

Tartu 2022

Investigation of Dopamine-mediated Toxicity in Parkinsonian Sensory Neuron

Abstract:

Background: L-3,4-Dihydroxyphenylalanine (L-DOPA) has stood as the gold-standard-treatment for PD and parkinsonism but its prolonged use has been linked to peripheral neuropathy in PD. This study investigates the impact of L-DOPA on sensory neuronal morphology and mitochondrial function in sensory neurons treated with rotenone, a pesticide associated with increased risk of development of PD in humans.

Methods: DRG sensory neurons were treated with different concentrations of rotenone (1nM, 10nM, 100nM and 500nM). These cells were also treated with L-DOPA at concentrations that mimic those reported in patient plasma (3μM, 30μM, 300μM). Control cells were treated with vehicles. Cells were treated for 24 hours in hypoxic conditions (3% O2) to mimic the endogenous environment of sensory neurons in vivo, and parallel cultures were treated and cultured in normoxia (21% O2). Mitochondrial membrane potential and oxidative stress were determined using TMRM and DHE assays, respectively. In addition, neuronal morphology was analysed based upon beta-III tubulin immunoreactivity.

Results: At the low concentrations of rotenone used, which are more relevant to modelling PD, no change in mitochondrial membrane potential was observed. Moreover, little change in betaIII tubulin immunoreactivity was observed between groups, suggesting that the concentrations used of rotenone and of L-DOPA were not overtly toxic at this time point. Oxidative stress is thought to play a key role in the toxicity of both rotenone and L-DOPA, and neurons treated with rotenone only did show increased oxidative stress in normoxic conditions. However, little oxidative stress was observed in rotenone-treated neurons cultured in hypoxic conditions. In neurons treated with L-DOPA only, we also observed increased oxidative stress in normoxic conditions when compared with hypoxic conditions. When DRGs were co-treated with rotenone and L-DOPA and cultured in normoxic conditions, additive effects were observed whereby more oxidative stress was observed in cells treated with both compared with cells treated with either, or neither. Very little oxidative stress was observed in neurons cultured in hypoxic conditions and treated with both agents.

Conclusions: Hypoxia, which is actually normoxia when compared with the in vivo environment, reduces the ability of rotenone to induce oxidative stress in vitro. Oxygen tension also plays a key role in the toxicity of L-DOPA in vitro. These results emphasise the importance of accurate modelling of the in vivo environment.

Keywords: Sensory neuropathy, L-DOPA, rotenone, dorsal root ganglion cells

CERCS: B640 Neurology, neuropsychology, neurophysiology

Kokkuvõte

Dopamiini vahendatud toksilisus parkinsonismi mudeldavates sensoorsetes neuronites.

Abstrakt:

Taust: L-3,4-Dihüdroksüpfenüülalaniini (*ingl keeles* L-3,4-Dihydroxyphenylalanine, L-DOPA) manustamist Parkinsoni haiguse ja parkinsonismi ravil on käsitletud kuldstandardina, kuid selle pikaajalist kasutamist on seostatud Parkinsoni haigusega kaasneva perifeerse neuropaatia tekkega. Käesolev uurimistöö uurib L-DOPA efekti sensoorsete neuronite morfoloogiale ja mitokondrite funktsioonile, mudelis, kus rakke on eelnevalt töödeldud rotenooniga, pestitsiidiga, mis on tõendatult inimestel Parkinsoni haiguse kujunemisega seotud riskifaktor.

Meetodid: Dorsaaljuure ganglioni neuroneid (*ingl keeles* dorsal root ganglion, DRG) mõjutati erinevate rotenooni kontsentratsionidega (1nM, 10nM, 100nM ja 500nM) või ka L-DOPA-ga kontsentratsioonidel, mis mimikeerivad selle patsientide plasmast leitud koguseid (3µM, 30µM, 300µM). Kontrollrakke mõjutati vastavate kemikaalide kandjalahustega. Rakke hoiti 24 tundi hüpoksilites tingimustes (3% O2), et mimikeerida sensoorsete neuronite endogeenset keskkonda *in vivo* ning paralleelkultuure kasvatati normoksia seisundis (21% O2). Mitokonrdiaalse membraani potensiaali ja oksüdatiivse stress taset jälgiti kasutades vastavalt TMRM ja DHE katsesüsteemi. Lisaks anaüüsiti rakkude neuronaalset morfoloogiat beta-III tubuliiini immunoreaktiivsuse abil.

Tulemused: Suhteliselt madalatel rotenooni kontsentratsioonidel, mis on asjakohased mudeldamaks Parkinsoni haigust, ei leitud mõju rakkude mitokondrite membraanipotensiaalile. Erinevates gruppides täheldati rakkude beta- III tubuliini immunreaktiivsuse signaalile ainult vähest mõju, mis viitab, et kasutatud rotenooni ja L-DOPA kontsentratsioonid ei põhjustanud rakkudel valitud ajapunktis toksilist efekti. L-DOPA ja rotenooni vahendatud toksilisuse peapõhjuseks peetakse oksüdatiivset stressi kujunemist rakkudes. Kui normoksia tingimustes, ainult rotenooniga töödeldud neuronites, täheldati suurenenud oksüdatiivse stressi olemasolu, kuid hüpoksilises keskkonnas oli rotenooniga töödeldud neuronites täheldatav vähene oksüdatiivse stressi tõus. Neuronites, mida töödeldi ainult L-DOPA-ga, oli normoksilites tingimustes oksüdatiivse stressi tase kõrgem võrreldes neuronitega, mida oli hoitud hüpoksilites tingimustes. Kui DRG neuroneid mõjutati nii rotenooni kui L-DOPA-ga üheaegselt ja kasvatati neid seejärel normoksia tingimustes, leiti nende ainete mõju osas aditiivne efekt võrreldes rakkudega, mida oli töödeldud vaid ühega neist ainetest või kui rakud olid jäetud töötlemata. Väga vähest oksüdatiivset stressi täheldati neuonites, mida kasvatati hüpoksilites tingimustes ja töödeldi mõlema ainega.

Järeldused: Hapniku tase mängib võtmerolli L-DOPA toksilisusel *in vitro*. Hüpoksia, mis on tegelikkuses normoksia, kui seda võrrelda *in vivo* keskkonnaga, vähendab rotenooni võimet

indutseerida oksüdatiivset stressi *in vitro*. Need tulemused rõhutavad rakukultuuride *in vivo* keskkonna korrektse mudeldamise olulisust.

Võtmesõnad: sensoorne neuropaatia, L- DOPA, rotenoon, dorsaaljuure ganglion rakud.

CERCS: B640 Neuroloogia, neuropsühholoogia, neurofüsioloogia

TABLE OF CONTENTS

TERMS, ABBREVIATIONS AND NOTATIONS

3-OMD: 3-O-methyldopa

5,10‑CH2‑THF: 5,10‑methylenetetrahydrofolate

6-OHDA: 2,4,5- trihydroxy-phenethylamine

Ara-C: Arabinocytidine hydrochloride

ATP: Adenosine triphosphate

DA: Dopamine

DBS: Deep brain stimulation

DHE: Dihydroethidium

DMSO: Dimethyl sulfoxide

DRG: Dorsal root ganglion

ER: Endoplasmic reticulum

Glu: Glutamate

IPD: idiopathic Parkinson’s disease

L-DOPA: L-3,4-Dihydroxyphenylalanine

LB: Lewy body

LRKK2: leucine-rich repeat kinase 2

MPTP: 1,2,3,6-methyl-phenyl-tetrahydropyridine

Paraquat: N, N′-dimethyl-4-4-4′-bipyridinium

PD: Parkinson’s disease

PINK1: PTEN-induced putative kinase 1

PN: Peripheral neuropathy

ROS: Reactive oxygen species

SNpc: Substantia nigra pars compacta

TH: Tyrosine hydroxylase

TMRM: Tetramethylrhodamine, methyl ester

UPDRS: Unified Parkinson's Disease Rating Scale

α‑syn: Alpha-synuclein

INTRODUCTION

Parkinson disease (PD) is a neurodegenerative disorder, second only to Alzheimer's disease in terms of its prevalence; it is known to affect 2 – 3% of the population who are ≥ 65 years of age (Poewe et al., 2017). The neuropathological hallmark of PD is the loss of neurons in the substantia nigra pars compacta (SNpc), causing a deficiency in dopamine, and Lewy bodies, which are intracellular inclusions of α- synuclein. Although neither alone are specific for PD, when present together, they are definitive for idiopathic Parkinson disease (IPD) (Poewe et al., 2017).

In prodromal PD, pain and sensory losses are seen before motor disturbances, it was reported in 106 parkinsonian patients that 60 – 70% of patients had to deal with varying degrees of acute or chronic pain such as neuropathic, dystonic pain, and headache (Zambito Marsala et al., 2011). These observations pointed out that sensory neurons are vulnerable in PD (Silverdale et al., 2018). Sensory neuropathy in PD is in the form of loss of olfactory function (Bohnen et al., 2010), combined with loss of thermal perception, pathological heat pain and mechanical hypersensitivity (Nolano et al., 2008). Phosphorylated alpha-synuclein (p-α-Syn), a pathological hallmark of PD once thought to be only present in the brain of PD patients, has been confirmed in dermal nerve fibres in IPD and suggested as a useful biomarker and diagnostic tool in IPD (Donadio et al., 2014). The deposition of p-α-Syn in skin sympathetic nerve fibres could further distinguish IPD patients from patients suffering from multiple system atrophy (MSA) and essential tremor. Another study suggested that p-α-Syn in IPD is preferentially deposited in autonomic fibres in contrast to somatosensory fibres in MSA (Doppler et al., 2015). Transcriptomic analysis of PD patients' skin has also revealed

important genes and pathways that are crucial to understand the molecular mechanisms and potential biomarkers of PD (Planken et al., 2017).

Animal and epidemiological studies have shown that repeated exposure to pesticide is a major risk factor of PD (Hancock et al., 2008). There is a 2.5 times likelihood that humans chronically exposed to rotenone will develop Parkinsonian-like symptoms compared to the general population (Innos & Hickey, 2021). Rotenone is a naturally occurring plant-derived toxin that is used as pesticides and piscicides. It is highly lipophilic thereby readily crosses the blood brain barrier without using the dopamine transporter. It inhibits complex I of the mitochondrial electron transport chain (mitochondrial NADH-dehydrogenase), increasing the production of reactive oxygen species (ROS) leading to oxidative stress and ultimate neurodegeneration (Betarbet et al., 2000).

Of all the pharmacological agents, L-3,4-Dihydroxyphenylalanine (L-DOPA) is the gold-standard for treatment of PD and parkinsonism. Practically all patients with PD will require L-DOPA treatment (LeWitt & Fahn, 2016). Peripheral neuropathy (PN) in PD may be impacted by the prolonged use of L-DOPA in patients, resulting in increased levels of homocysteine (Hcy) and methylmalonic acid (MMA). The surge in Hcy and MMA is from the metabolism of L-DOPA via the O-methylation pathway (Rajabally & Martey, 2013). However, there are opposing clinical studies linking PN in PD to the prolonged use of L-DOPA (Ceravolo et al., 2013; Conradt et al., 2018; Mancini et al., 2014; Shahrizaila et al., 2013). Moreover, L-DOPA is known to be a source of reactive oxygen species (Hörmann et al., 2021). In view of these discrepancies in the clinic, this study aims to examine the impact of L-DOPA on sensory neurons.

1 LITERATURE REVIEW

1.1 Parkinson's Disease Pathology

Parkinson disease (PD) is a neurodegenerative disorder, second only to Alzheimer's disease in terms of its prevalence; it is known to affect 2 – 3% of the population who are ≥ 65 years of age (Poewe et al., 2017). The neuropathological hallmark of PD is the loss of neurons in the substantia nigra pars compacta (SNpc), causing a deficiency in dopamine, and Lewy bodies, which are intracellular inclusions of α-synuclein. Although neither alone are specific for PD, when present together, they are definitive for idiopathic PD (Poewe et al., 2017).

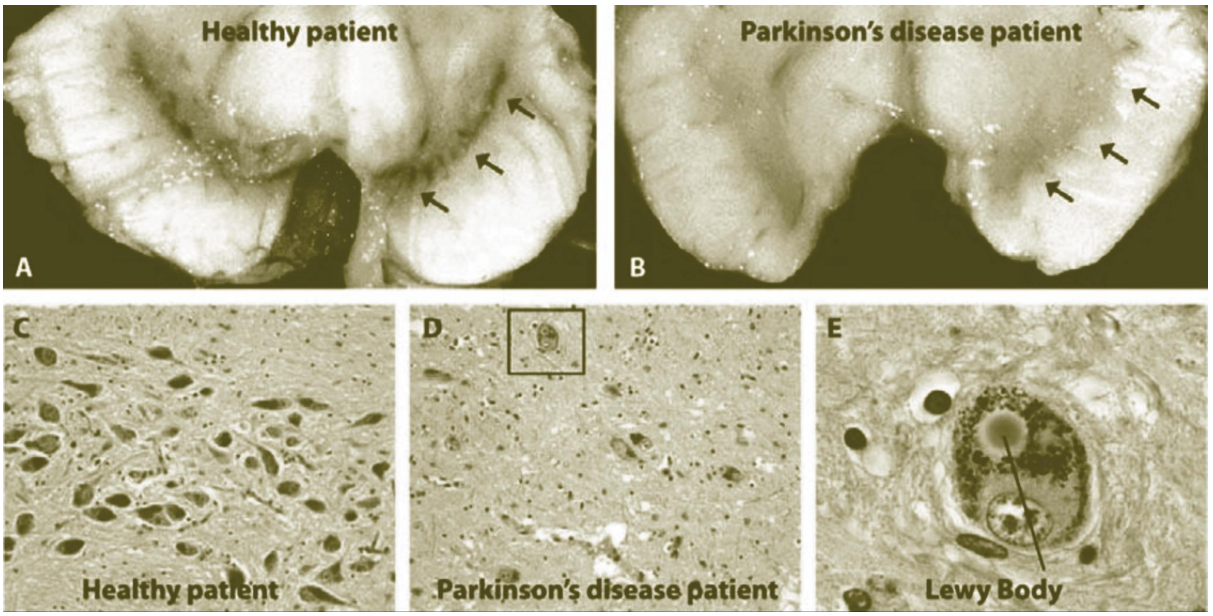

Fig. (1). *Pathological examination of a healthy individual (A) reveals typical pigmented dopaminergic (DA) neurons in the SNpc (arrows); in contrast, loss of SNpc neurons leads to pigment disappearance in the PD brain (B, arrows). Adapted from (Agamanolis, 2021).*

1.1.1 Symptoms of Parkinson's Disease

At the heart of a PD diagnosis is a defined motor syndrome, thus PD is clinically defined by the existence of bradykinesia in addition to either or both rigidity and rest tremor (Postuma et al., 2015). However, a combination of both motor and non-motor components is present in the early phase of PD, and more often, certain non-motor symptoms (NMS), such as olfactory loss (Haehner et al., 2011), loss of pain perception (M. Nolano et al., 2008) and constipation (M. Nolano et al., 2008) appear before the motor disorders are seen (Berg et al., 2015), (Chaudhuri & Schapira, 2009). Selected NMS including rapid eye movement sleep behaviour disorder, olfactory loss, urinary dysfunction, constipation, orthostatic hypotension, excessive daytime sleepiness, and depression constitute prodromal PD. Although these symptoms may coexist with PD motor signs, they are not specific to PD and they are insufficient for defining disease in prodromal state (Berg et al., 2015).

NMS affects a plethora of functions, including sleep (mainly sleep-wake cycle control, sleep-onset insomnia, rapid eye movement (REM) sleep behaviour disorder (RBD)), autonomic control (including orthostatic hypotension, urogenital dysfunction, constipation and hyperhidrosis), mood, sensation (mostly hyposmia and pain) as well as cognition (including frontal executive dysfunction, memory retrieval deficits, dementia and hallucinations) (Chaudhuri & Schapira, 2009).

Table 1. Motor and Non-motor Symptoms and Signs of PD

Symptoms	**Definition**
Motor	
Bradykinesia[p]	Slowness and decrease in automatic movement with difficulty in movement initiation
Rigidity[p]	Involuntary stiffness of the limbs resulting in decreased range of motion
Rest tremor[p]	A 4- to 6-Hz tremor present only when the limb is completely at rest but absent during movement
Postural instability	Trouble with balance and falls due to the inability to keep or modify postures when standing or walking; synonymous with late stage PD
Nonmotor	
Olfactory loss	Decreased or loss of sense of smell (hyposmia)
Sleep dysfunction	Symptoms of rapid eye movement sleep behaviour disorder, excessive daytime sleepiness, inability to stay asleep through the night (sleep-maintenance insomnia)
Autonomic dysfunction	Constipation, delayed gastric emptying (gastroparesis), urinary urgency and frequency, erectile dysfunction, orthostatic hypotension, inconsistent blood pressure
Psychiatric disturbances	Depression, anxiety, apathy, psychosis
Cognitive impairment	Mild cognitive impairment or dementia, often initially affecting attention, executive, and visuospatial functions
Other	Fatigue, hypophonia (softening of the voice), sialorrhea, difficulty in swallowing

[p] Indicates a primary feature.

Adapted from (Armstrong & Okun, 2020)

1.1.2 Management of Parkinson's Disease

The use of various dopaminergic pharmacotherapies remains the mainstay in the management of PD (Armstrong & Okun, 2020). Pharmacotherapy is predicated on the basis that the characteristic motor features of PD are a consequence of the depletion of striatal dopamine because of loss of dopaminergic neurons in the substantia nigra pars compacta (Poewe et al., 2017). The goal of pharmacotherapy intervention is to attenuate motor symptoms by restoring striatal dopaminergic tone, using dopaminergic agonists, monoamine oxidase B inhibitors and/or L-DOPA (plus carbidopa) (Connolly & Lang, 2014; Zeuner et al., 2019).

Of all the pharmacological agents, L-DOPA has stood as the gold-standard treatment for Parkinson disease and parkinsonism, and practically all patients with Parkinson disease will require L-DOPA treatment at one time or another (LeWitt & Fahn, 2016). However, off-target effects synonymous with systemic administration (such as nausea, drowsiness and orthostasis) and adverse on-target effects (for example, impulse control disorders) can be limiting, and complications (such as end-of-dose wearing off and dyskinesia) can emerge in the intermediate- and long-term (Antonini et al., 2018; Picconi et al., 2018). A key concern with L-DOPA is the continuous decline of the action time and "wearing off" of the therapeutic effect causing the manifestation of poorly controlled PD signs and symptoms before the next round of dosing (Parmar et al., 2020). There have been different pharmacological interventions to minimise the off-target effects namely, the use of adjuvant, fast-onset 'rescue' therapies in the form of a DA receptor agonist, such as apomorphine continuously administered as a subcutaneous infusion. In exceptional cases, intestinal delivery of L-DOPA-carbidopa gel may be used to provide a more continuous supply of L-DOPA.

Surgically, deep brain stimulation (DBS), can be used to implant unilateral or bilateral electrodes into a targeted area of the brain with the electrodes attached to an impulse generator (IPG) that will be placed in the chest using magnetic resonance imaging (MRI). The IPG acts as a pacemaker, providing impulse to the part of the brain involved in motor function, typically, the subthalamic nucleus or the internal globus pallidus. Upon DBS surgery, patients will attend routine consultations to access and optimise the stimulation frameworks and medications (Armstrong & Okun, 2020). DBS is used to mitigate motor symptoms, tremor, and dyskinesia that may arise from the wearing off of L-DOPA therapy (Fox et al., 2018). Results from a meta-analysis indicated an overall superiority of DBS over best medical therapy (BMT) in terms of improvement in impairment/disability, quality of life, and medication dose reduction (Bratsos et al., 2018). However, the study noted that there was no significant difference in L-DOPA equivalent dose (LED) reduction between early and advanced PD patients; and a higher risk of serious adverse events (SAE) (Bratsos et al., 2018).

Stem cell-based therapies, although still in research stage, have been reported to restore dopaminergic inputs to the striatum and are now being considered as a durable alternative to oral medications especially L-DOPA because of its off-target effects, wearing off and the challenges with timely dosing (Parmar et al., 2020).

1.2 Peripheral Neuropathy in Parkinson's Disease

Peripheral neuropathy (PN) is a general term that indicates any dysfunction in sensory, motor, and autonomic nerves of the peripheral nervous system (Paul et al., 2020). PN affects axons and/or myelin of nerve fibres (Wolfe et al., 1999). It may be inferred that the symptoms of PN

result from sensory neuron deterioration prior to motor neuron impairment, although motor impairment may be more prominent in neuropathies such as chronic inflammatory demyelinating neuropathy (Latov, 2002). The diverse causes of PN include metabolic and endocrine dysfunction, genetic diseases, HIV, infectious diseases, and thyroid disorder, with diabetes mellitus being the most common, accounting for 60% of PN in patients with diabetes (Simon, 2009). Also, other causes such as genetic mutations in certain genes, i.e., Parkin genes for PD, deficiency of vitamins B1, B6, B12 and folate have been linked with PN (Simon, 2009; Müller et al., 2013; Rajabally & Martey, 2013).

1.2.1 Neurophysiological Types of Neuropathy in PD and their Diagnosis

Neuropathy could be classified as mononeuropathy caused by trauma or entrapment by surrounding tissue; mononeuropathy multiplex commonly caused by leprosy and vasculitis; polyneuropathy when it involves many nerves due to toxic, metabolic or systemic aetiology (Misra et al., 2008) and ganglionopathies due to axonal loss in sensory ganglia (Marquez-Infante et al., 2013).

Neuropathy could also be classified as small fibre neuropathy (SFN) and large fibre neuropathy (LFN). SFN involves the unmyelinated C and the thinly myelinated Aδ fibres, it presents clinically as predominantly pain. Possible diagnostic criteria include length-dependent symptoms, clinical signs (pinprick and thermal sensory loss and/or allodynia/hyperalgesia) (Themistocleous et al., 2014). Precise diagnosis is based upon clinical signs of small fibre damage, nerve conduction studies, altered intra-epidermal nerve fibre density, and abnormal quantitative sensory testing (QST) (Themistocleous et al., 2014).

Skin biopsy has also shown to be precise in SFN diagnosis (Hlubocky et al., 2010). LFN, on the other hand, involves the Aα and Aβ myelinated fibres and can be diagnosed by nerve conduction studies (Zis et al., 2017).

In deciphering sensory neuropathy from motor neuropathy, sensory involvement should not include motor neuron disease; likewise, motor involvement should not include dorsal root ganglion neuropathy (Misra et al., 2008). However, mixed neuropathies are also observed.

1.2.2 Evidence to support Sensory Neuropathy in Parkinson's Disease

There are two recent reviews that have aggregated research outcomes on the possible connection between peripheral neuropathy and PD (Zis et al., 2017); (Paul et al., 2020). Zis et al., noted that most neuropathies in PD are sensory and are mostly distal, symmetrical, and axonal (Paul et al., 2020). In prodromal PD, pain and sensory losses are seen before motor disturbances; it was reported in 106 parkinsonian patients that 60 – 70% of patients with PD had to deal with varying degrees of acute or chronic pain such as neuropathic, dystonic pain, and headache (Zambito Marsala et al., 2011). These observations point out that sensory neurons are vulnerable in PD pathophysiology (Silverdale et al., 2018). Sensory neuropathy in PD also takes the form of loss of olfactory function (Bohnen et al., 2010), combined with loss of thermal perception, pathological heat pain and mechanical hypersensitivity (Nolano et al., 2008).

Clearer evidence that supports sensory neuropathy in PD can be noted from skin biopsies of PD patients, which shows a preponderance of SFN and mixed-fibre polyneuropathies (Nolano et al., 2008) consistent with pathological QST findings. These neuropathies could

also be observed with corneal confocal microscopy as swollen axon, compensatory fibre sprouting, and α-synuclein aggregates in cutaneous sensory and autonomic nerves (Podgorny et al., 2016); (Nolano et al., 2017). A parallel pattern has also been noted in motor neurons in genetic and idiopathic PD models of rodents (Vivacqua et al., 2009) and indeed, PD patients show loss of sensory neurites in skin over time (Vacchi et al., 2021).

Phosphorylated alpha-synuclein (p-α-Syn) is a promising candidate biomarker of IPD because of its presence in the dermal nerve fibre in IPD. The usefulness of p-α-Syn as a diagnostic tool for IPD was first tested by (Donadio et al., 2014). In that study, 21 patients with well characterised IPD and 20 patients with parkinsonism (PAR) assumed not to have p-α-Syn deposits (vascular parkinsonism 10, tauopathies 6, parkin mutations 4) alongside with age-matched healthy controls were enlisted in the study. Skin biopsy from cervical skin sites (proximal) and thigh and leg sites (distal) were used to study p-α-Syn deposits and small nerve fibres. They observed that there was no p-α-Syn deposit in any skin sample in PAR patients and controls but present in the cervical skin sites of all the IPD patients. They therefore concluded that p-α-Syn can be a positive biomarker in the diagnosis of IPD in the proximal peripheral nerve and can also distinguish between IPD and PAR (Donadio et al., 2014). Similarly, the deposition of p-α-Syn in skin sympathetic nerve fibres could further distinguish IPD patients from patients suffering from multiple system atrophy (MSA) and essential tremor. Another study suggested that p-α-Syn in IPD is preferentially deposited in autonomic fibres in contrast to somatosensory fibres in MSA (Doppler et al., 2015).

Moreover, transcriptomic analysis on skin biopsies of 12 PD patients and matched controls revealed over 1000 differentially expressed genes (DEGs) and pathways related to signal transduction, nuclear regulation, mitochondrial function, immune response, and protein metabolism (Planken et al., 2017). The principal DEGs are important in biological function

and development of PD. Therefore, RNA-seq is crucial to understand the molecular mechanisms and potential biomarkers of PD.

Table 2. Peripheral manifestations of PN in PD

Manifestations of PN in PD	Functional changes	Pathological changes	References
Cutaneous neuropathy	Seborrhoea, hyperhidrosis, impaired wound healing, skin homeostasis, nuclear processes and tumorigenic pathways	Cutaneous denervation and α-synuclein deposits in dermal somatosensory and autonomic nerve fibres	(Doppler et al., 2014), (Wang et al., 2013), (Planken et al., 2017)
Sensory neuropathy	Increase in tactile and thermal thresholds together with a reduction in mechanical pain perception	Impairment of mitochondrial respiration, deregulation of transient receptor potential channels (TRPV) and (TRPA) at mRNA protein functional levels in DRGs, significant loss of epidermal nerve fibres and Meissner corpuscles, accumulation of glycosylceramides (GlcCer) in the DRGs and accumulation of α-synuclein in the DRGs and spinal nerves	(Nolano et al., 2008), (Valek et al., 2021)

1.3 Models for Investigating Parkinson's Disease

Modelling is important for studying symptoms, signs, mechanisms and treatment modalities of neurodegenerative diseases. However, models must show construct, face and predictive validity (Tadenev & Burgess, 2019).

Different animal models of PD have emerged to promote the exploration of the aetiology and treatment of PD. Currently, most PD research has utilised toxin-induced and genetic animal models (Hisahara & Shimohama, 2011). The role played by environmental toxins and genetic factors in sporadic PD are becoming clearer (Tanner et al., 2011); (Gilks et al., 2005).

In the neurotoxic models, substances that cause both reversible (reserpine) and irreversible (MPTP, 6-OHDA, paraquat, rotenone) neurotoxic effects are administered to model animals while genetic models target some known genetic risk factor or causes in PD patients (SNCA (α‑syn, PARK1, and 4), PRKN (parkin RBR E3 ubiquitin-protein ligase, PARK2), PINK1 (PTEN-induced putative kinase 1, PARK6), DJ‑1 (PARK7), and LRRK2 (leucine-rich repeat kinase 2, PARK8) to develop PD effect (Chesselet & Richter, 2011)

1.3.1 Neurotoxin-induced Animal Models of PD and their Mechanisms

Neurotoxic compounds such as MPTP (1,2,3,6-methyl-phenyl-tetrahydropyridine), 6-OHDA (2,4,5-trihydroxy-phenethylamine), rotenone, paraquat (N, N′-dimethyl-4-4-4′-bipyridinium), paraquat used with manganese ethylenebis-dithiocarbamate (Maneb), result in the degeneration of dopaminergic neurons in animals (Tieu, 2011). These neurotoxins inhibit mitochondrial complex I and accelerate oxidative stress (Penttinen et al., 2016).

A summary of four toxin models of PD and their properties is shown in the table below.

Table 3. Summary of toxin-induced PD mouse models and their properties.

Model	Administration / Pathology	Mechanism	Response to L-DOPA
6-OHDA	Administered as microinjections into discrete areas of the brain Nigrostriatal damage seen in substantia nigra cell bodies, striatal terminals, and striatal dopaminergic neurons	1. Generation of ROS and ultimately, oxidative stress-related cytotoxicity 2. Inhibits electron transport chain complex I 3. Microglia activation	Yes
MPTP	Administered systemically as sc injections. Nigrostriatal damage seen in substantia nigra cell bodies, striatal terminals, and striatal dopaminergic neurons with conflicting reports on α-synuclein accumulation	1. Metabolised to MPP^+ which induces neurotoxicity primarily by inhibiting complex I of the mitochondrial electron transport chain, resulting in ATP depletion and increased oxidative stress 2. Microglia activation	Yes
Rotenone	Administered systemically or as microinjections into discrete areas of the brain Nigrostriatal damage seen in substantia nigra cell bodies, striatal terminals, and striatal dopaminergic neurons including α-synuclein accumulation	1. ROS production leading to oxidative stress 2. Inhibit electron transport chain complex I	Yes
Paraquat	Administered systemically or as microinjections into discrete areas of the brain. Nigrostriatal damage mainly seen in substantia nigra cell body, and aggregation of α-synuclein in mouse brain	1. ROS production leading to oxidative stress 2. Inhibit electron transport chain complex I	Yes

Abbreviations: ROS Reactive oxygen species. MPP^+ 1-methyl-4-phenylpyridinium

1.4 Dorsal Root Ganglion (DRG) Function in Homeostasis and Neuropathic Pain

The dorsal root ganglia (DRG) are found in the peripheral nervous system (PNS). The cell bodies of these sensory neurons are located close to the spinal cord. They are pseudo-unipolar neurons that innervate peripheral target organs and transduce sensory input to the central nervous system (CNS) via the dorsal horn of the spinal cord. At the spinal cord, the ascending primary neuron synapses with secondary sensory neurons in order to propagate sensory impulses to the higher CNS structures (Basbaum et al., 2009).

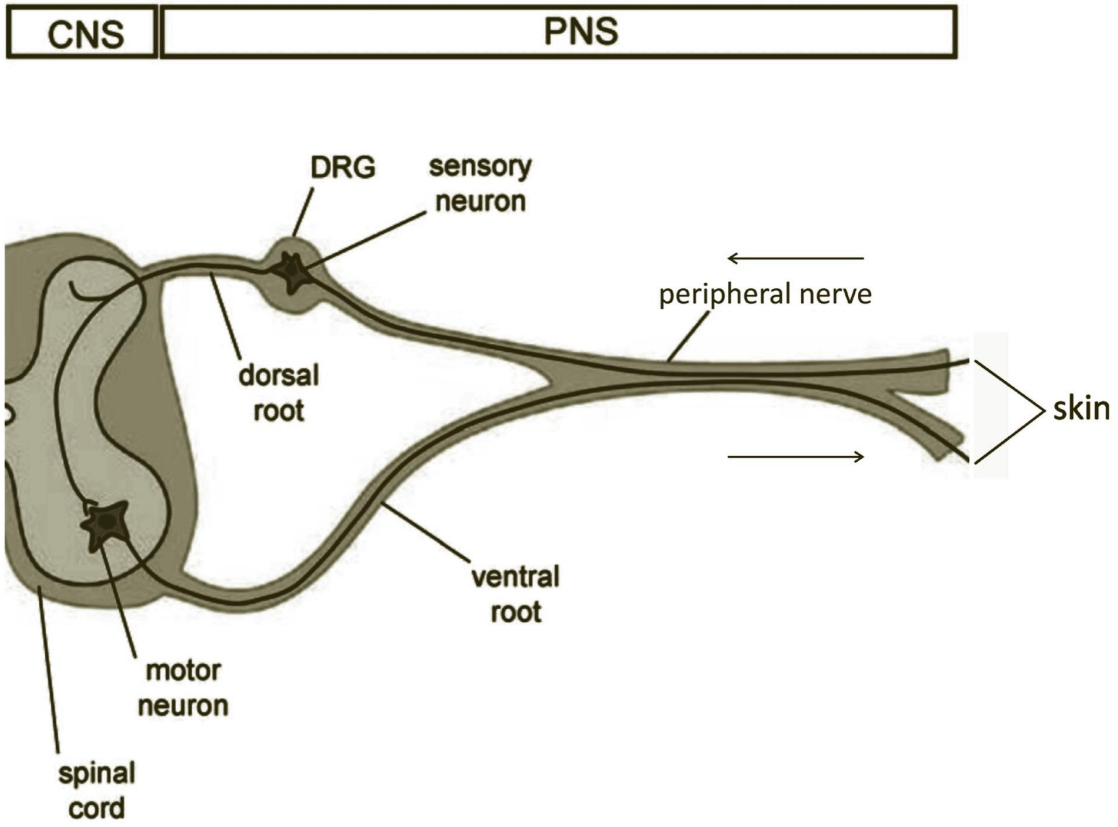

Fig. (2). *Schematic representation of sensory-motor neuron circuitry and the location of the DRG (Geeven Gert, 2010).*

DRG neurons mediate diverse sensations because of expression of different channels, receptors, and unique morphological features. This also allows the discrimination of different types of sensations (Platika et al., 1985).

Table 4. DRG neurons are responsible for distinct sensory modalities.

Sensation	**DRG neuron responsible**	**Reference**
Proprioception and mechanoreception (e.g., touch)	Conducted by low threshold, fast conducting, myelinated Aα and Aβ fibres DRG neurons with large cell bodies	(Berta et al., 2017)
Nociceptive pain	Transmitted by either thinly myelinated medium-velocity Aδ fibres or unmyelinated slow-conducting C-fibres most requiring high activation threshold	

DRG signalling is suggested to be involved in the incidence and perpetuation of neuropathic pain (Krames, 2014). An in vivo analysis of DRG neurons revealed that 85% of them are modality-specific in normal conditions but become polymodal under pathological conditions such as after tissue inflammation or injury (Emery et al., 2016). In the aftermath of an injury, the DRG experiences a tremendous change in structure and function, and these plastic alterations initiate the DRG as the site of propagation of pain signals migrating to the brain (Liu et al., 2000).

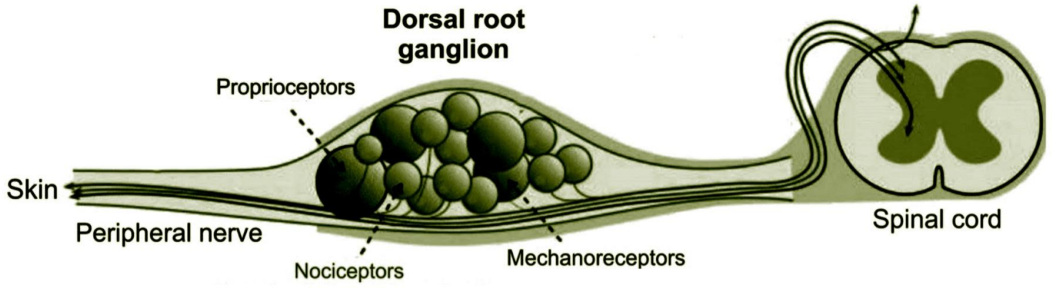

Fig. (3). DRG neurons showing receptors for distinct sensory modalities. Adapted from (Berta et al., 2017)

1.5 Dopamine therapy in Parkinson's disease and its association with Peripheral Neuropathy

PN in PD may be impacted by the prolonged use of L-DOPA in patients. L-DOPA and indeed, DA itself, have long been postulated as sources of reactive metabolites. For example, both are metabolised to reactive quinones by tyrosinase (Meiser et al., 2013), an enzyme present in skin (Eisenhofer et al., 2003), or L-DOPA can be auto-converted to reactive quinones (Hörmann et al., 2021).

Moreover, L-DOPA may lead to increased levels of homocysteine (Hcy) and methylmalonic acid (MMA). The surge in Hcy and MMA is from the metabolism of L-DOPA via the O-methylation pathway (Rajabally & Martey, 2013).

The figure below shows the metabolic pathway of L-DOPA and how prolonged use could result in the accumulation of these metabolites.

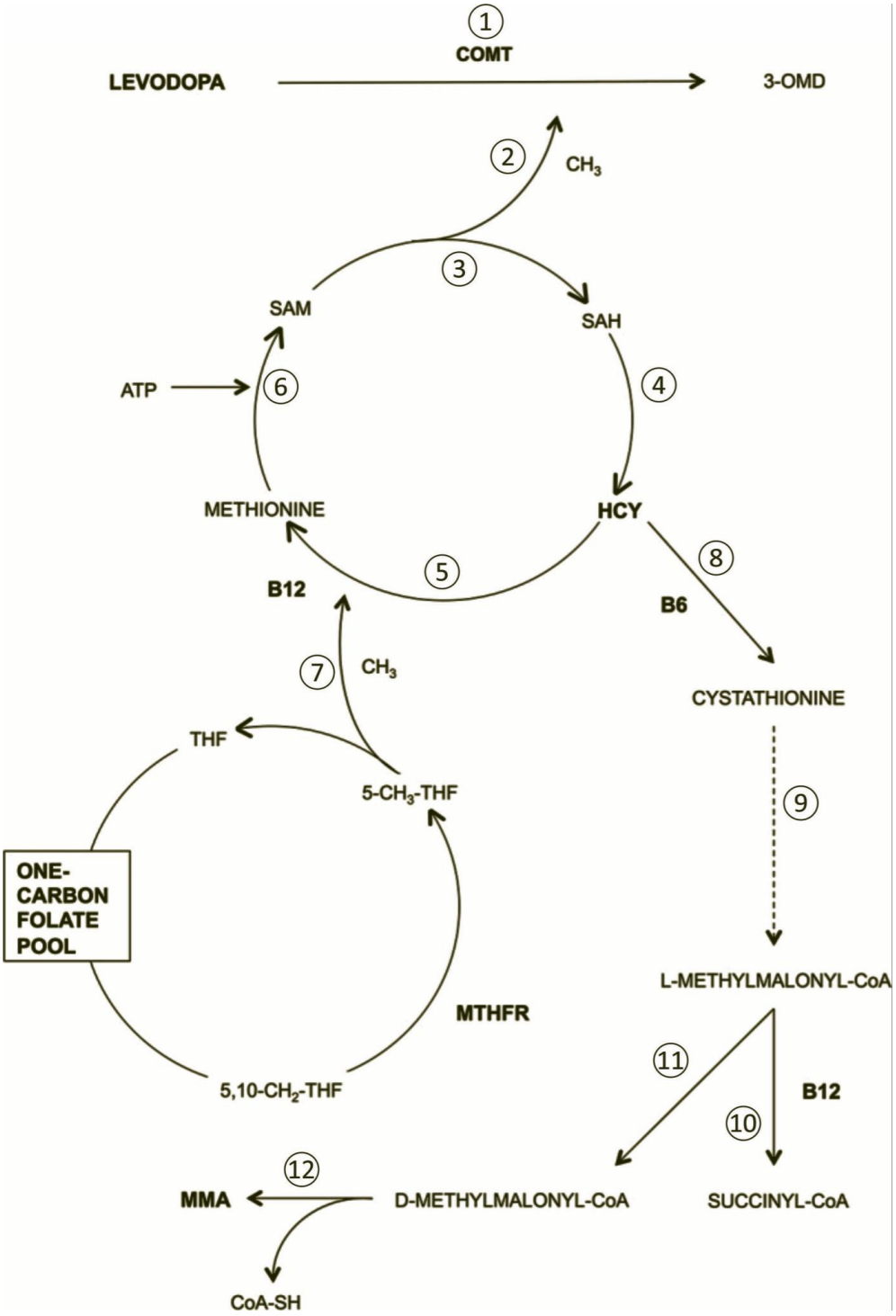

Fig. (4). *L-DOPA metabolic pathway.*

Abbreviations: 3-OMD, 3-O-methyldopa; 5,10-CH2-THF, 5,10-methylenetetrahydrofolate

Adapted from: (Romagnolo et al., 2018)

L-DOPA is converted into 3-O- methyldopa (3-OMD) by Catechol-O- methyltransferase (COMT) **(1)** using the methyl group donated by S-adenosylmethionine (SAM) **(2)**. On donating the methyl group, SAM converted into S- adenosylhomocysteine (SAH) **(3)** and then, almost immediately into homocysteine (HCY) **(4)** (Müller et al., 2013), (Rajabally & Martey, 2013).

HCY will normally be re-methylated into methionine **(5)** and SAM **(6)** by methyl-tetrahydrofolate (THF) and B12 **(7)** or converted into cysteine via irreversible transsulfuration **(8)** (Rajabally & Martey, 2013). However, SAM is depleted in the methylation of L-DOPA resulting in increased plasma level of homocysteine (Müller et al., 2013). Consequently, prolonged use of L-DOPA can result in the buildup of Hcy and MMA, as well as to exhaustion of vitB6, vitB12, and folate (Romagnolo et al., 2019).

Elevated levels of Hcy and MMA is assumed to be caused by the deficiency of vitamin B12, which is a vital cofactor for the conversion of homocysteine to methionine and SAM. Cobalamin's role as a cofactor for the isomerization of succinyl-CoA **(10)** also makes its deficiency a reason for MMA accumulation **(12)** (Müller et al., 2013); (Rajabally & Martey, 2013).

A multicentre study had shown elevated Hcy and MMA levels in PD patients compared with control, with notable increase in patients with longer L-DOPA usage (Ceravolo et al., 2013). In the study, the risk of neuropathy in PD patients and the role played by L-DOPA dosage were evaluated. The risk of neuropathy in patients with (> 3 years) L-DOPA exposure was 19.4%, only 6.8% of patients with (< 3 years) L-DOPA developed neuropathy while only 4.82% without L-DOPA exposure were found to show neuropathy among the 330 PD patients used in the study (Ceravolo et al., 2013). Similarly, among the 137 healthy controls with similar age spread, 8.76% were diagnosed with axonal neuropathy, notably involving sensory

neurons (Ceravolo et al., 2013). It was also observed that there was a reduced plasma level of vitamin B12 but a significant increase in Hcy and MMA levels among the patients with long term L-DOPA treatment (Ceravolo et al., 2013).

This study also observed that the risk of neuropathy went up by 8% every year, implying that age is also an important factor in PN in PD and not only the length of time of L-DOPA administration (Ceravolo et al., 2013). Although in an age-controlled study, it was reported that age is not a determinant factor for neuropathy in PD but age-related vitamin B12 in addition to other age-related nutrient deficiency are involved (Rajabally & Martey, 2013).

However, there is growing evidence that provides a contrary narrative about the involvement of L-DOPA in PN. A 2.4-fold higher prevalence of PN in PD was reported in a cohort study of over 5,000 L-DOPA naive PD patients observed against 20,000 non-parkinsonian controls (Conradt et al., 2018). Furthermore, other studies involving mostly asymptomatic using electromyogram (EMG) to confirmed PN reported ranges from 4.8% to 24.0% including in L-DOPA naive PD patients (Mancini et al., 2014; Shahrizaila et al., 2013; Ceravolo et al., 2013).

In view of these discrepancies in the clinic, we aim to examine the impact of L-DOPA on sensory neurons.

2 THE AIM OF THE THESIS

We aim to investigate the impact of L-DOPA on sensory neuronal morphology and mitochondrial function in sensory neurons treated with rotenone.

3 EXPERIMENTAL PART

3.1 MATERIALS AND METHODS

3.1.1 Materials

Table 4. Specifications of the antibodies used.

Product name and description	Company	Code
Normal Goat Serum	Jackson ImmunoResearch	005-000-121
Normal Donkey Serum	Jackson ImmunoResearch	017-000-121
Alexa Fluor® 594-AffiniPure Goat Anti-Rabbit IgG (H+L)	Jackson ImmunoResearch	111-585-003
Fluorescein (FITC) AffiniPure Goat Anti-Mouse IgG (H+L)	Jackson ImmunoResearch	115-095-146
Anti-beta III Tubulin antibody (Rabbit polyclonal to beta III Tubulin) - Neuronal Marker	Abcam	ab18207
Alexa Flour 488-AffiniPure Donkey Anti-chicken IgY (IgG) (H+L)	Jackson ImmunoResearch	703-545-155
Anti-MAP2 antibody (Chicken polyclonal to MAP2)	Abcam	ab5392
Anti-ATP Synthase Antibody, β chain, clone 4.3E8.D1	Sigma Aldrich	MAB3494

3.1.2 DRG neuronal cultures

5-10-day-old rat pups were euthanized by decapitation, and dorsal root ganglia from the thoracic to lumbar regions were isolated and digested with collagenase (Thermofisher) and DNAse at 37° C for 45 min. After 3 hours, the digested DRG neurons were plated onto Cell Vis 4-chamber glass-bottom dishes in 500µL Neurobasal-A medium (Gibco) supplemented

with B-27 (Thermofisher), gentamicin (krka) and glutamine (Thermofisher). After 24 hours, cells were treated with 1.5 μM of Ara-C (Sigma Aldrich) to reduce the proliferation of fibroblasts. They were incubated at 37° C in 5% CO_2 for one week before exposure to hypoxia, treatment with rotenone and L-DOPA.

3.1.3 Rotenone and L-DOPA treatments

After one week of incubation, the cells were transferred into a hypoxic chamber where they were left for 3 days to acclimatise to 3% O_2, 5% CO_2 and 92% N_2. After 3 days, the cells were treated for 24 hours with rotenone (Sigma Aldrich) (1nM, 10nM, 100nM and 500nM, 1x4-quadrant plate per treatment). Cells were also treated with L-DOPA methyl ester (Sigma Aldrich; a more water-soluble form of -LDOPA; 3μM, 30μM, 300μM) or vehicle, one quadrant per rotenone treatment, i.e., for the plate treated with 0nM rotenone, 1 quadrant was treated with L-DOPA vehicle, 1 quadrant was treated with 3μM, 1 quadrant was treated with 30μM, and 1 quadrant was treated with 300μM, so on for other rotenone-treated plates. Vehicle controls for rotenone and L-DOPA were DMSO (Sigma Aldrich) and distilled water, respectively. Additional plates of cells, treated in parallel, were incubated in normoxia (5% CO_2, 20% O_2). After 24 hours after treatment, membrane potential and oxidative stress assays were performed. Cells were then fixed for 10 minutes in 4% paraformaldehyde (Sigma Aldrich) containing 250mM of sucrose (Fisher Bioreagent) and stored at -4° C for subsequent immunostaining.

3.1.4 Measurement of membrane potential

Membrane potential was examined via TMRM (Thermofisher). For this assay, all cells were removed to normoxia, loaded with 10 nM TMRM in new complete medium for 30 min at 5% CO_2 and 37°C in the dark and imaged with a confocal microscope (LSM780, ex 561nm, em 566-669nm;). Using ImageJ software, the confocal images were analysed by determining the

mean pixel intensity of each outlined soma.

3.1.5 Oxidative stress assay

Dihydroethidium (DHE) (Santa Cruz Biotechnology) was used to measure the reactive oxygen species (ROS) level in live target cells. ROS generation is determined by total DHE fluorescence intensity. All cells were removed to normoxia, and 1 µl of 10 µM DHE was added to cells in 500 µl of their treatment medium and incubated for 30 minutes. Imaging was conducted using confocal microscopy (LSM780, ex 561nm, em 585-733nm). Subsequently, the images were analysed with ImageJ using particle analysis. Briefly, images were thresholded using manual intensity threshold boundaries of 120-255. Particle sizes were limited to 200 micron^2 -infinity, and circularity set at 0.10-1.00, to ensure that only DRG neurons were quantified and to avoid the fibroblasts present in our mixed cultures. Importantly, DRGs grow on top of the fibroblasts, and imaging was carefully selected to image only these DRGs, providing an additional method to avoid signal interference from fibroblasts.

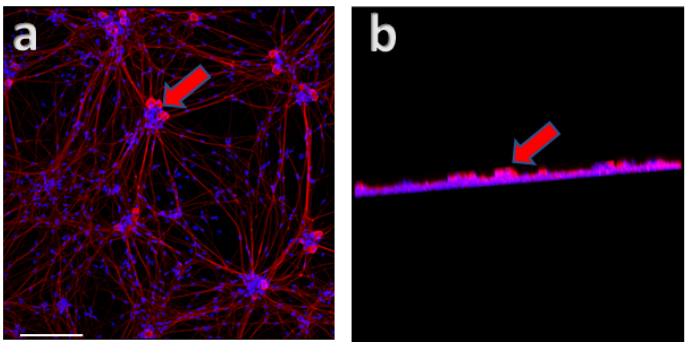

Fig. (5). 3D image of DRG neurons growing on top of fibroblasts. *(a) Top view of DRG neurons stained with beta-III tubulin (red) and Hoechst-34580 stains (blue) (b) Side view of DRG neurons stained with beta-III tubulin (red) and Hoechst-34580 stains. Arrows pointing at DRG neurons on top. Scale bar in (a) = 250µm*

3.1.6 Immunostaining

The fixed cells were treated with 0.1% Triton X-100 (Sigma Aldrich) for 10 minutes and then in block (4% goat serum (Jackson ImmunoResearch) in 0.01M PBS) for 1 hour. After 1 hour, they were incubated overnight with primary antibodies; anti-beta-III tubulin (Abcam) diluted to 1:2500 in block and anti-ATP5B (Sigma Aldrich) diluted to 1:500 in block. The following day, cells were processed as follows: cells were washed in PBS for 3×5 minutes each and then incubated for 2 hours in secondary antibodies diluted to 1:200 in block; goat anti-rabbit (Jackson ImmunoResearch) for beta-III tubulin and goat anti-mouse (Jackson ImmunoResearch) for ATP5B. Then, cells were washed again in 3× PBS for 5 minutes each and stained with 0.5 μg/ml Hoechst-34580 dye (Sigma Aldrich) for 5 minutes. Cells were washed a further two times in PBS and a drop of fluorescence mounting added. Cells were imaged using a confocal microscope (LSM780, ex 561nm em 585-733nm for beta-III tubulin and ex 405nm em 410-499nm for Hoechst-34580). Similarly, ImageJ was used to quantify the percentage area of neurons using the best performing auto-threshold.

For MAP2 immunostaining, methanol was used for permeabilization. Methanol was added to the 4% paraformaldehyde-fixed cells for 10 minutes in -20^{o}C. The steps are similar to the beta-III tubulin staining. Specifically, 1:500 primary antibody, anti-MAP2 (Abcam) was used and secondary antibody, donkey anti-chicken (Jackson ImmunoResearch), was diluted to 1:200 in block (5% donkey serum).

3.1.7 Statistics

Data analysis and graphing was performed using GraphPad V9.3.1. Data are presented as means ± standard deviation. Unpaired t-tests were used for comparison between two groups. Where data showed different variances, Mann-Whitney U tests were used for comparisons between two groups. Two-way ANOVAs (mixed-effects model) followed by appropriate

post-hoc tests were used to compare data where there were two factors, e.g., rotenone treatment and L-DOPA treatment. p values < 0.05 were considered significant.

3.2 RESULTS

3.2.1 Determining the appropriate concentration of rotenone to use in DRG cells to model idiopathic PD

We began our experiments with a preliminary study on the concentration of rotenone for inducing idiopathic Parkinsonism. The morphology of the neurons was examined using MAP2 immunostaining. [MAH1] There was a trend towards a dose-dependent effect of rotenone over a 7 day period as shown in the decrease in percentage area of MAP2 at 500nM and 1μM by 7 days in **fig. (6)**, however, this effect did not reach significance (effect of treatment F (5, 18) = 2,204, p=0.09.) due to variability within treatment groups. **Fig. (7)** shows the confocal images of the neuron at different concentrations of rotenone (1nM - 1μM) using MAP2.

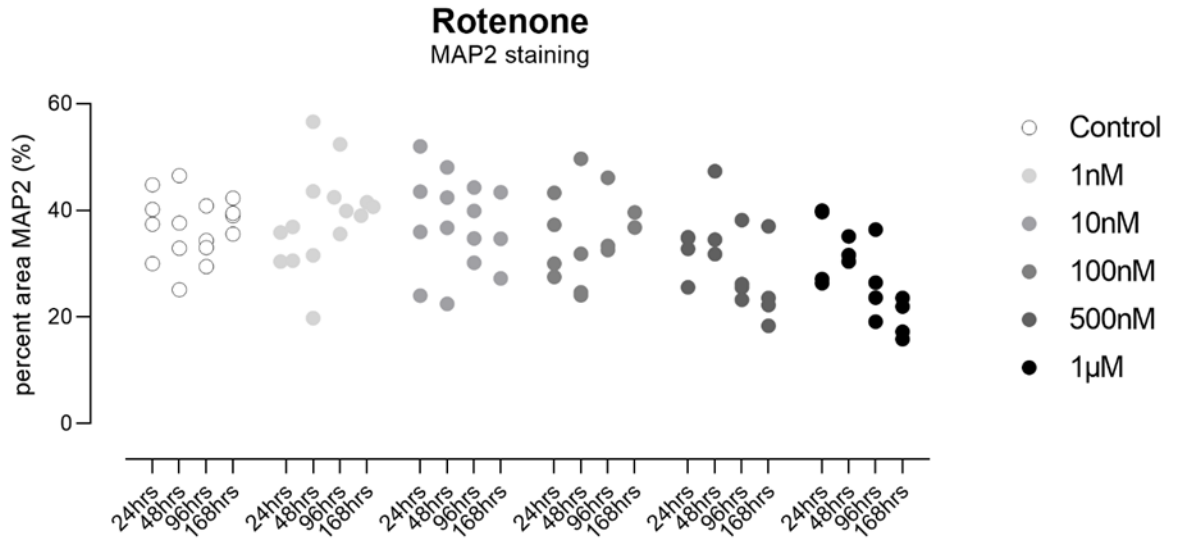

Fig. (6). Dose-dependent effect of rotenone on DRG neurons over a duration of 168 hours.

Data from individual quadrants (each data point is the mean percent MAP2-stained per quadrant) from each of four separate experiments are shown. N = 4 biological replicates.

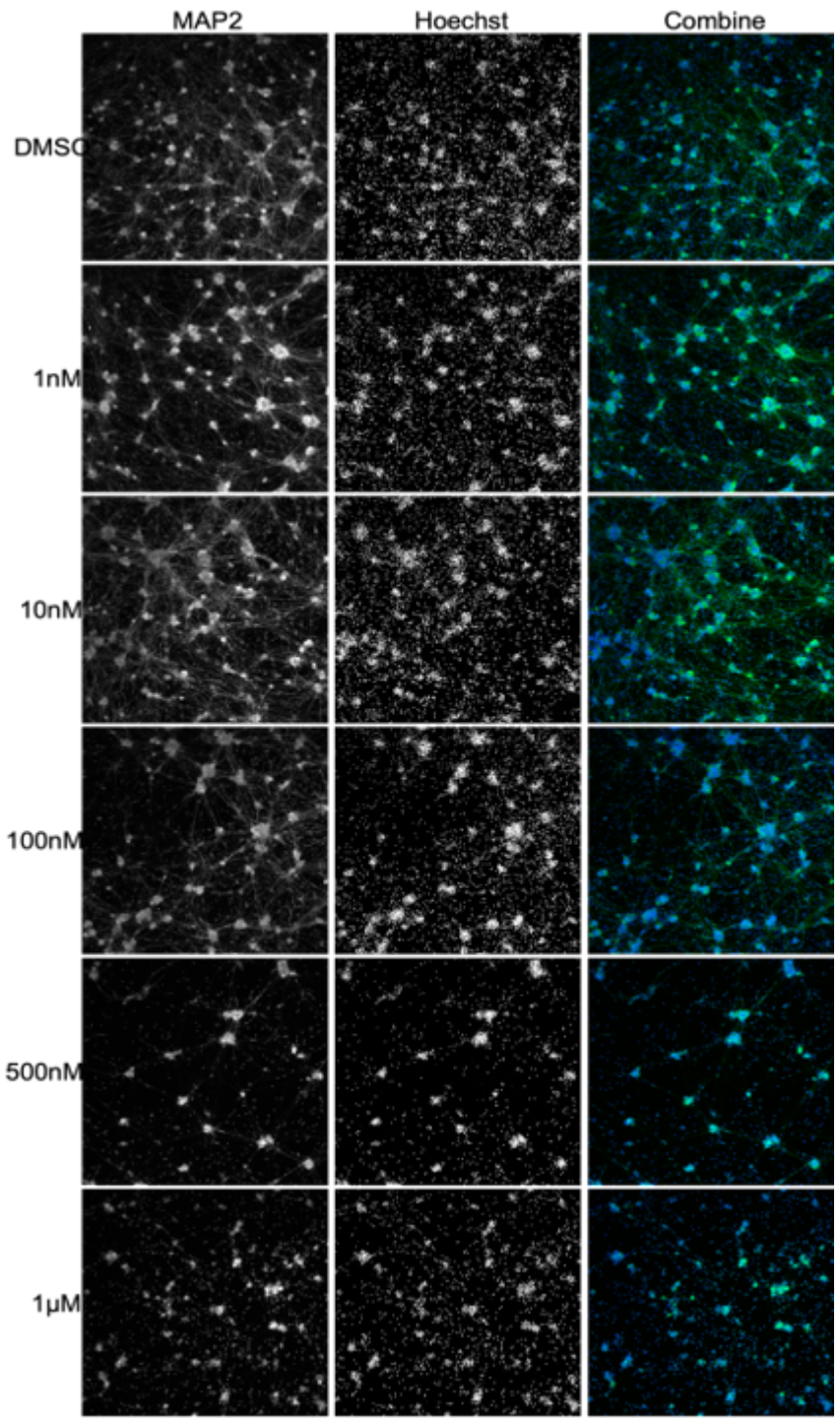

Fig. (7). Images of DRG neurons upon rotenone treatment after 168 hours

Shown are representative images of different concentrations of rotenone on DRG.

Single-channel images are shown in black and white for improved contrast.

Scale bar = 200µm.

We observed in our study that MAP2, although widely used as a neuronal marker, was not specific in staining sensory neurons in DRG cells. Signals came from the fibroblasts also (although we used AraC, our cultures were mixed). This would pose a challenge in subsequent analyses. Consequently, we switched to the use of beta-III tubulin as a neuronal marker, which showed more specificity in its ability to detect sensory neurons without including signals from fibroblasts. In **fig. (8)**, we show how this non-specific staining (a) is picked up in thresholding during analysis (b) and could lead to reduced sensitivity in cytotoxicity experiments. In **fig. (9)**, we compare beta-III tubulin (top) staining with MAP2 staining (bottom). Whether cells were treated with vehicle (a, c) or rotenone (b, d), beta-III tubulin staining was more specific for DRGs than MAP2 and was selected for further experiments.

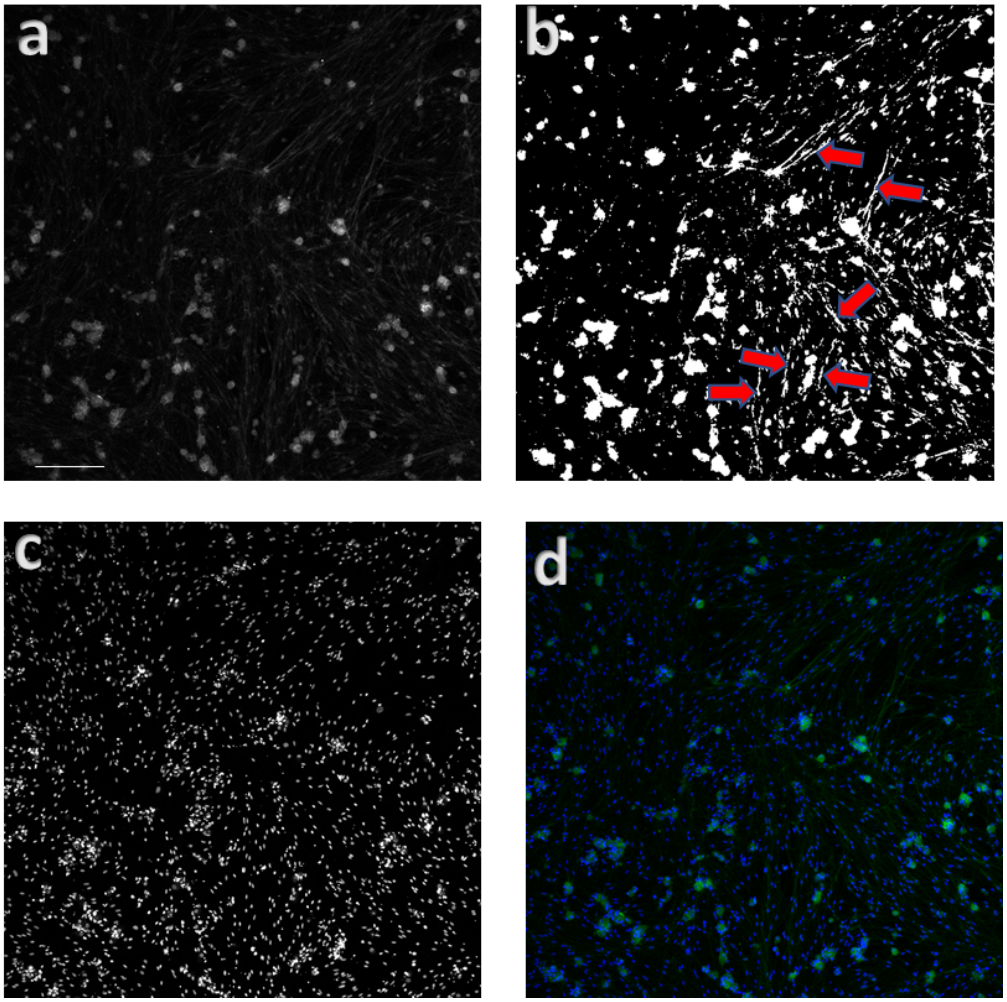

Fig. (8). Issues with MAP2 staining in DRG neurons. *Representative images of DRGs treated with 100nM rotenone and stained with MAP2 after 48hrs. (a) DRG neurons stained for MAP2 and (b) thresholded for analysis. Arrows in b show signals from fibroblasts in the thresholded image. (c) Cells were stained for MAP2 and Hoechst was also used to reveal nuclei. This image shows the Hoechst staining from (a). Hoechst-34580 stains all cells (DRGs + fibroblassts). (d) Merged channel images of (a) and (c). Scale bar in (a) = 100μm*

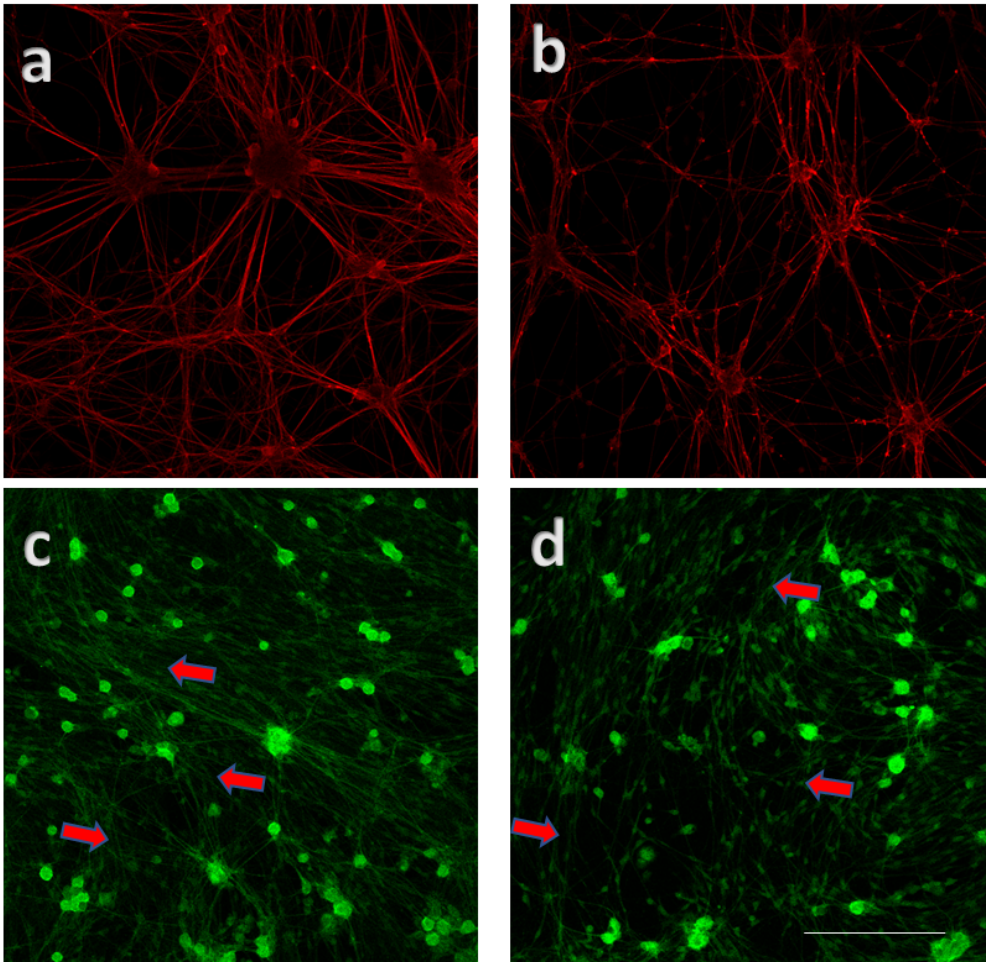

Fig. (9). Images comparing beta-III tubulin with MAP2 staining. *Cells were treated with vehicle (a, c) or 500 nM rotenone (b, d) for 48hrs. (a) DRG neurons stained with beta-III tubulin at 0 nM rotenone in hypoxia after 48 hrs. (b) DRG neurons stained with beta-III tubulin at 500 nM rotenone in hypoxia after 48 hrs (c) DRG neurons stained with MAP2 following treatment with DMSO (control) for 48 hrs. Arrows show fibroblasts (d) DRG neurons stained with MAP2 following treatment with 500 nM rotenone for 48 hrs. Arrows showing fibroblasts. Scale bar = 250μm.*

3.2.2 Effect of oxygen on oxidative stress induced by rotenone and L-DOPA in hypoxia and normoxia

Oxidative stress in the DRG cells was analysed after rotenone and L-DOPA incubation in normoxia and hypoxia for 24 hours. Oxidative stress is reported as the intensity of fluorescence of DHE by the DRG cell bodies, which was expressed as percent area (area within region of interest (ROI) divided by total area). There is ROS formation during L-DOPA auto-oxidation in a normoxic environment, previously described by (Ren et al., 2019) but oxygen tension in neuronal cells under physiological conditions is only 0.5-5% (Erecińska & Silver, 2001). This is why we are examining the effect of L-DOPA under hypoxic conditions, which mimics the endogenous environment of DRGs (Carreau et al., 2011) and enhances the translational value of our rotenone model of IPD. ROS production is represented as total fluorescence and was significantly elevated in normoxic culture compared to cells in hypoxia indicating oxidative stress in normoxia.

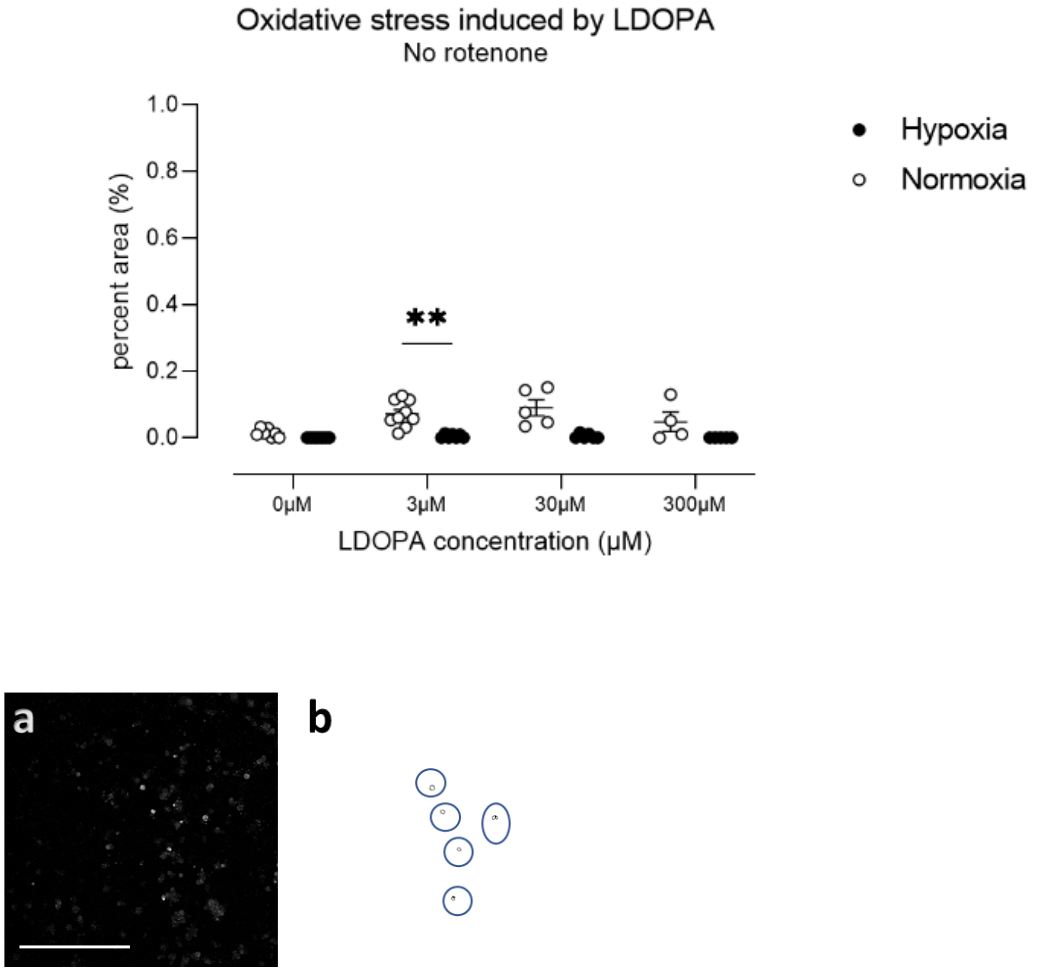

Fig. (10). Oxidative stress induced by L-DOPA in hypoxic and normoxic culture. *DRG neurons were treated with 3μM, 30μM and 300μM L-DOPA or distilled water and cultured in normoxic or hypoxic conditions. The graph shows a representative experiment and data points show data from several regions of interest with a particular treatment quadrant. Effect of L-DOPA treatment F (2,078, 29,09) = 4,728; p = 0.0157. Effect of oxygen F (1, 42) = 39,76; p < 0,0001. Effect of L-DOPA treatment + Oxygen F (3, 42) = 3,537; p = 0.0226. Šídák's multiple comparisons test was used to compare hypoxia and normia at 3μM L-DOPA **p < 0.01. (a) Representative image of DRG neurons emitting oxidised DHE-derived fluorescence (b) Manually thresholded image (neurons within blue circles) on ImageJ. Scale bar = 250 μm.*

L-DOPA induced more oxidative stress in normoxic conditions compared with hypoxic conditions (Figure 9). There was also a visible colour change in the medium of the normoxia groups at 24 hours after incubation with 300 μM L-DOPA, indicating auto-oxidation of L-DOPA into quinones, other toxic metabolites and neuromelanin **fig. (11)**.

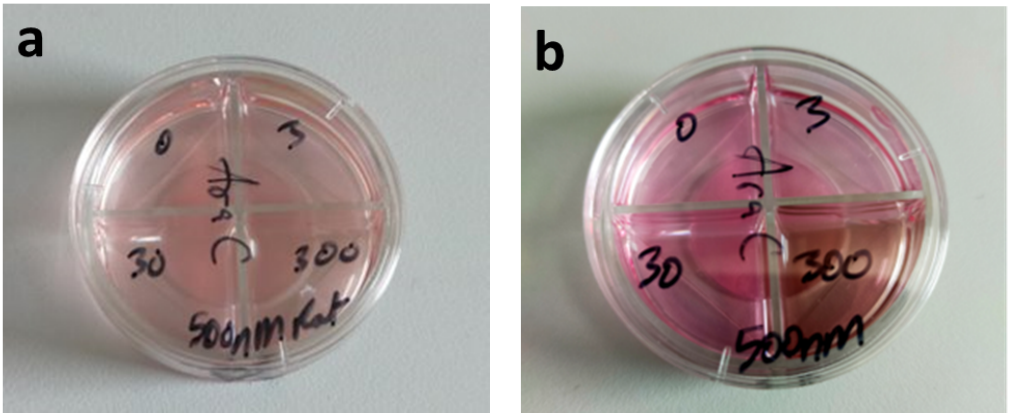

Fig. (11). Colour change in medium as a result of L-DOPA oxidation in normoxia. *(a) DRG neurons at 24 hours post-treatment with L-DOPA in hypoxia (b) DRG neurons 24 hours post-treatment with L-DOPA in normoxia.*

We also studied the effect of different concentrations of rotenone alone (1nM, 10nM, 100nM and 500nM) on the DRG cells in the absence of L-DOPA in both normoxia and hypoxia. There was a significant effect of rotenone on oxidative stress in the normoxic DRG neurons after 24 hours of treatment, which was not seen in hypoxia **fig. (12)**.

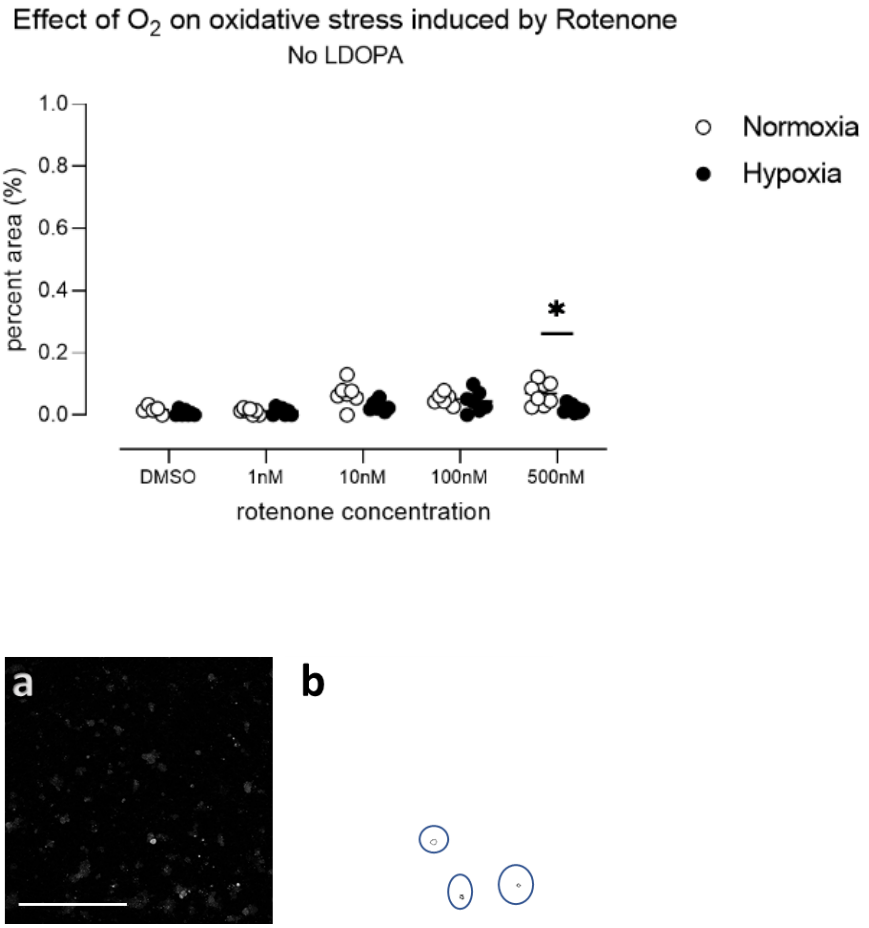

Fig. (12). Oxidative stress induced by rotenone in hypoxic and normoxic conditions. *DRG neurons were treated with rotenone (1nM, 10nM, 100nM and 500nM) or DMSO as control and cultured in hypoxic or normoxic conditions. The graph shows a representative experiment and data points show data from several regions of interest with a particular treatment quadrant. Effect of rotenone treatment F (2,841, 31,96) = 11,09; p <0,0001. Effect of oxygen F (1, 14) = 9,124; p = 0,0092. Effect of rotenone treatment + Oxygen F (4, 45) = 3,624; p = 0,0121. Šídák's multiple comparisons test was used to compare hypoxia and normia at 500 nM rotenone *p = 0,0264. (a) Representative image of DRG neurons emitting oxidised DHE-derived fluorescence (b) Manually thresholded image (neurons within blue circles) on ImageJ. Scale bar = 250 μm.*

.

Critically, we compared the effects of normoxia and hypoxia on the overall effects of rotenone and L-DOPA combinations. Our results showed that L-DOPA and rotenone treatment was additive, with increased oxidative stress observed in normoxia compared with either drug alone or neither drug **fig. (13)**. However, very little oxidative stress was observed in hypoxia **fig. (14)**. We note that the vastly increased DHE fluorescence observed at 100nM Rotenone and 30μM L-DOPA was not a consistent result; but it is nevertheless shown for completeness.

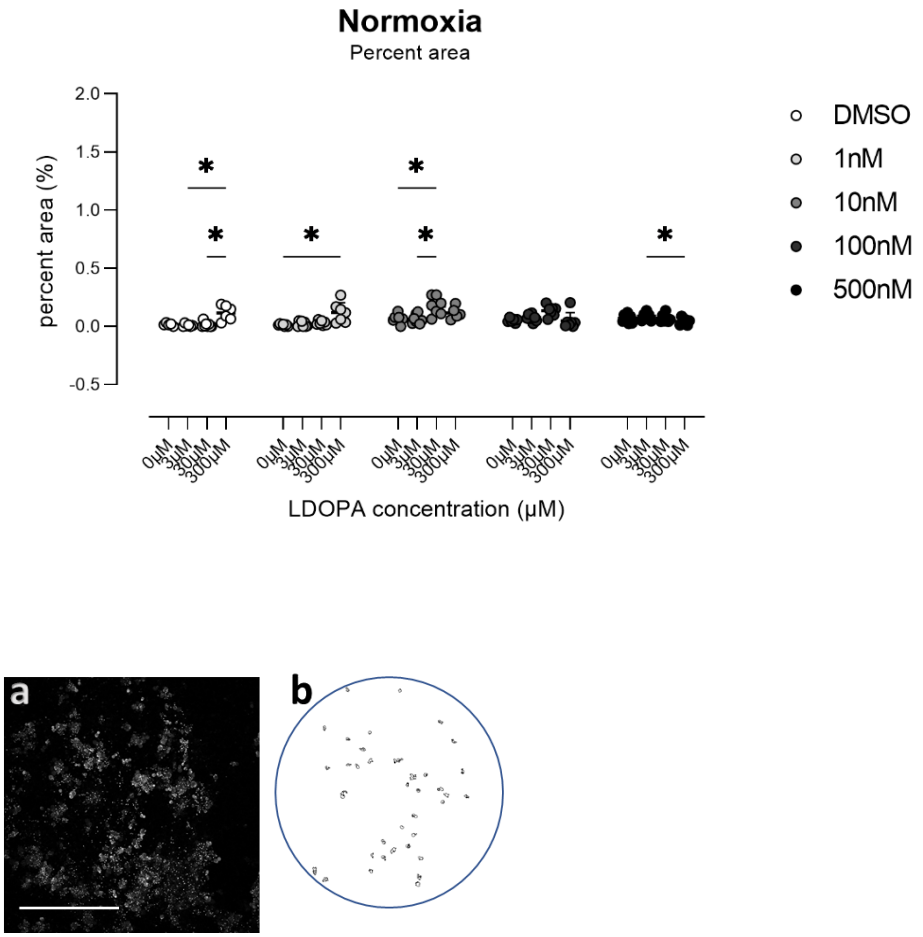

Fig. (13). Effect of normoxia on oxidative stress induced by combinations of rotenone and L-DOPA in DRG neurons. *DRG neurons were treated with rotenone (1nM, 10nM, 100nM, 500nM) or DMSO as control and also 3µM, 30µM or 300µM L-DOPA or distilled water as control. The graph shows a representative experiment and data points show data from several regions of interest with a particular treatment quadrant. Effect of rotenone treatment F (4, 35) = 9,019; p < 0,0001. Effect of L-DOPA F (1,836, 49,58) = 9,204; p = 0,0006. Effect of rotenone + L-DOPA treatment F (12, 81) = 6,683; p < 0,0001. Tukey's multiple comparisons test was used to compare between and within different groups. 3µM vs. 300µM L-DOPA (DMSO) *p = 0,0416; 30µM vs. 300µM L-DOPA (DMSO) *p = 0,0408; 0µM vs. 300µM L-DOPA (1 nM rotenone) *p = 0,0443; 0µM vs. 30µM L-DOPA (10 nM rotenone) *p = 0,0350; 3µM vs. 30µM L-DOPA (10 nM rotenone) *p = 0,0302; 3µM vs. 300µM L-DOPA (500 nM rotenone) *p = 0,0213 (a) Representative image of DRG neurons emitting oxidised DHE-derived fluorescence (b) Manually thresholded image (neurons within blue circle) on ImageJ. Scale bar = 250 µm.*

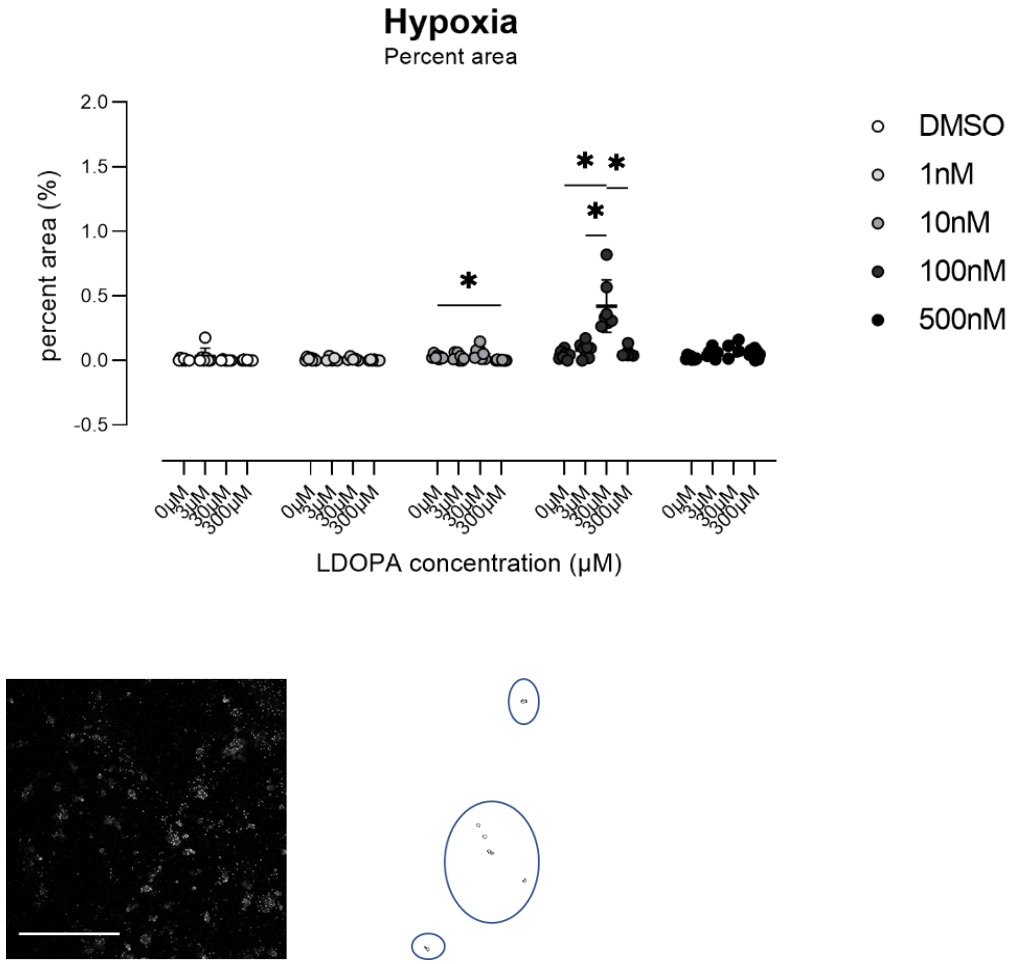

Fig. (14). Effect of hypoxia on oxidative stress induced by combinations of rotenone and L-DOPA in DRG neurons . *DRG neurons were induced with rotenone (1nM, 10nM, 100nM and 500nM) or DMSO as control and treated with 3µM, 30µM and 300µM L-DOPA or distilled water as control for L-DOPA. The graph shows a representative experiment and data points show data from several regions of interest with a particular treatment quadrant. Effect of rotenone treatment F (4, 119) = 30,96; p <0,0001. Effect of L-DOPA F (1,406, 55,76) = 19,64; p <0,0001. Effect of rotenone + L-DOPA treatment F (12, 119) = 13,55; p < 0,0001. Tukey's multiple comparisons test was used to compare between and within different groups. 0µM vs. 300µM L-DOPA (10 nM rotenone) *p = 0,0151; 0µM vs. 30µM L-DOPA (100 nM rotenone) *p = 0,0126; 3µM vs. 30µM L-DOPA (100 nM rotenone) *p = 0,0265; 30µM vs. 300µM L-DOPA (100 nM rotenone) *p = 0,0350. (a) Representative image of DRG neurons emitting oxidised DHE-derived fluorescence (b) Manually thresholded image (neurons within blue circle) on ImageJ. Scale bar = 250 µm.*

Our results from two biologic replicates (Table 5) were consistent and showed that L-DOPA causes oxidative stress in normoxia, and that when combined with rotenone, shows additive effects. However, very little oxidative stress was observed in hypoxic conditions following treatment with L-DOPA, with rotenone or with combinations of them both. However, at high concentrations of both L-DOPA and rotenone, consistent significant effects were lost (Table 5, 500nM rotenone). In future experiments, we shall follow these cells over longer time periods. We hypothesise that cells treated with high concentrations of rotenone and L-DOPA die earlier than DRGs treated with lower concentrations and it is possible that timepoints than 24hrs would be required to observe oxidative stress in these extreme conditions in normoxia.

Table 5. Comparing normoxia versus hypoxia in two biological replicates

Condition	Expt. / Conc. of rotenone	P value	P value summary	Statistically significant (P < 0,05)?	F (DFn, DFd)
Normoxia Vs Hypoxia	#1 at 1 nM	0,0031	**	Yes	F (1, 13) = 13,15
	#2 at 1 nM	0,0001	***	Yes	F (1, 46) = 17,12
Normoxia Vs Hypoxia	#1 at 10 nM	< 0,0001	****	Yes	F (1, 51) = 49,71
	#2 at 10 nM	-	-	-	-
Normoxia Vs Hypoxia	#1 at 100 nM	0,0021	**	Yes	F (1, 48) = 10,57
	#2 at 100 nM	< 0,0001	****	Yes	F (1, 12) = 33,65
Normoxia Vs Hypoxia	#1 at 500 nM	0,2931	ns	No	F (1, 15) = 1,187
	#2 at 500 nM	0,0063	ns	No	F (1, 43) = 8,243

As a positive control for DHE staining, we examined the effect of H_2O_2 on DRGs cultured in normoxia. This is important to validate our outcome measure. As shown in **figs. (15),** DRGs showed increased ROS formation after 4 hour treatment with 200 μM H_2O_2 compared to treatment with 0.01M PBS.

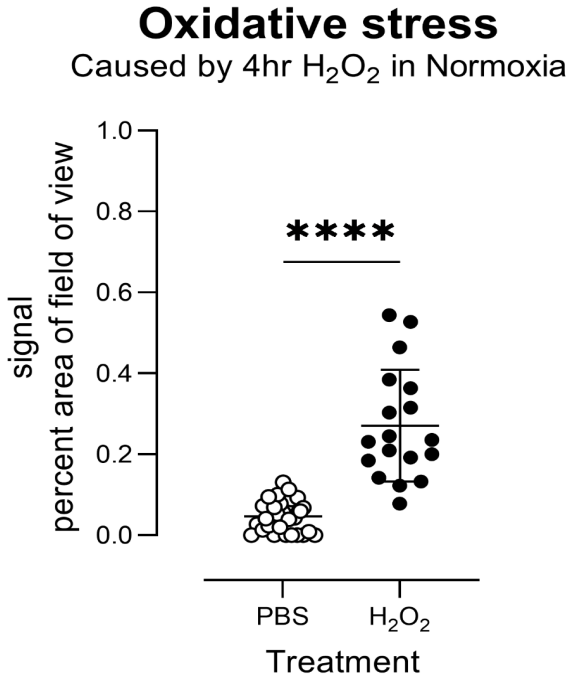

Fig. (15). Positive control for DHE. *DRGs cultured in normoxia were treated with 200 μM H_2O_2 for 4 hours and imaged as before, for oxidised DHE. H_2O_2-treated cells show increased ROS formation, based upon imaging of fluorescent DHE. Data show regions of interest with a particular treatment quadrant. N=1 experiment. Data were compared using a Mann-Whitney U test, $p<0.0001$.*

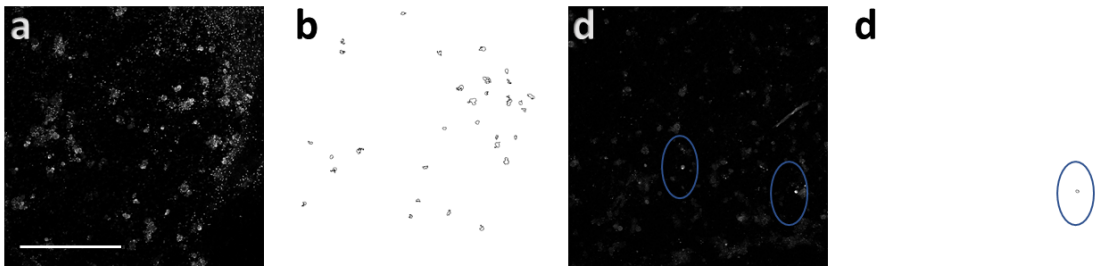

Fig. (16). Oxidative stress caused by H_2O_2 in normoxia and comparison between normoxia and hypoxia with PBS 4 hour post-treatment. *Cells were treated with 200 µM H_2O_2 or 0.01M PBS then incubated for 4 hours. At 4 hours, cells treated with 200 µM H_2O_2 (a) showed significant oxidative stress compared to control-treated cells (d). See Figure 13 for graph.. (a) DRG neurons treated with 200 µM H_2O_2 (b) DRG neurons treated with 200 µM H_2O_2 upon analysis on ImageJ (c) DRG neurons treated with 0.01M PBS (d) DRG neurons treated with 0.01M PBS upon analysis on ImageJ. Blue circle shows the thresholded "particles". Scale bar = 250 µm*

3.2.3 Response of DRG neurons mitochondrial membrane potential to rotenone and L-DOPA

This assay was performed on DRG cells cultured in hypoxia after incubation with rotenone and L-DOPA for 24 hours. Both rotenone and L-DOPA cause oxidative stress, rotenone via inhibition of complex I. Nevertheless, the formation of reactive oxygen species by very mild inhibition of electron cycling via complex I is thought to be more important for IPD than profound inhibition of ATP formation by the mitochondrial electron transport chain (Innos and Hickey 2021). The aim of this assay was to investigate whether mitochondria were perturbed by these low concentrations of rotenone. Healthy cells with functional

mitochondria will show bright signals, which become dim or cease with the loss of mitochondrial membrane potential because TMRM is not able to accumulate in the mitochondria (fig. 16). The mean soma pixel intensity for DRGs treated with combinations of rotenone and L-DOPA from 3 experimental replicates show a stable mean TMRM intensity without any significant difference between groups, as shown in **fig. (18)**.

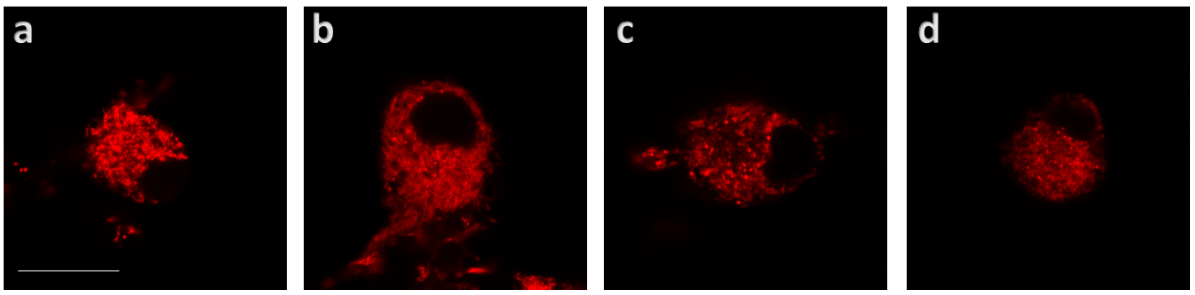

Fig. (17). Visualisation of TMRM signal in DRG neurons cultured in hypoxia and treated with rotenone and with L-DOPA at 24 hours post-treatment*. (a) A DRG neuron stained with TMRM following treatment with 500 nM rotenone and 0 μM L-DOPA in hypoxia after 24 hrs (b) A DRG neuron stained with TMRM following treatment with 500 nM rotenone and 3 μM L-DOPA in hypoxia after 24 hrs (c) A DRG neuron stained with TMRM following treatment with 500 nM rotenone and 30 μM L-DOPA in hypoxia after 24 hrs (d) A DRG neuron stained with TMRM following treatment with 500 nM rotenone and 300 μM L-DOPA in hypoxia after 24 hrs. Scale bar = 250 μm*

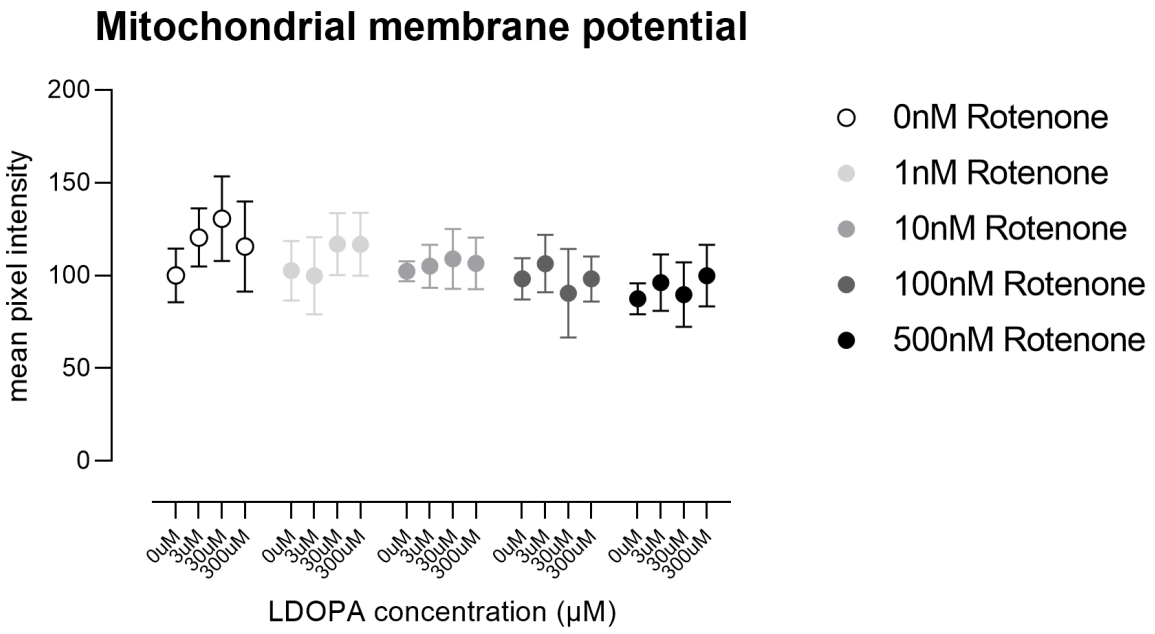

Fig. (18). Mean pixel intensity of TMRM-stained mitochondria in DRG soma following treatment with different concentrations of rotenone and L-DOPA. *Rotenone and L-DOPA treatment did not cause any significant change in membrane potential. Data shown are the mean ± sem of n = 3 independent experiments. Data were analysed using ANOVA (L-DOPA x Rotenone F(12, 30)=1,119, ns) followed by Tukey's multiple comparisons test.*

We set up a positive control experiment form TMRM using 100 µM FCCP, as a mitochondrial oxidative phosphorylation uncoupler. Our result in (fig. 18) showed there was a decrease in mean pixel intensity confirming impairment in mitochondrial membrane potential activity. These data confirm our ability to detect mitochondrial membrane potential damage in DRG cells upon treatment and that neither L-DOPA nor rotenone caused significant change in mitochondrial membrane potential.

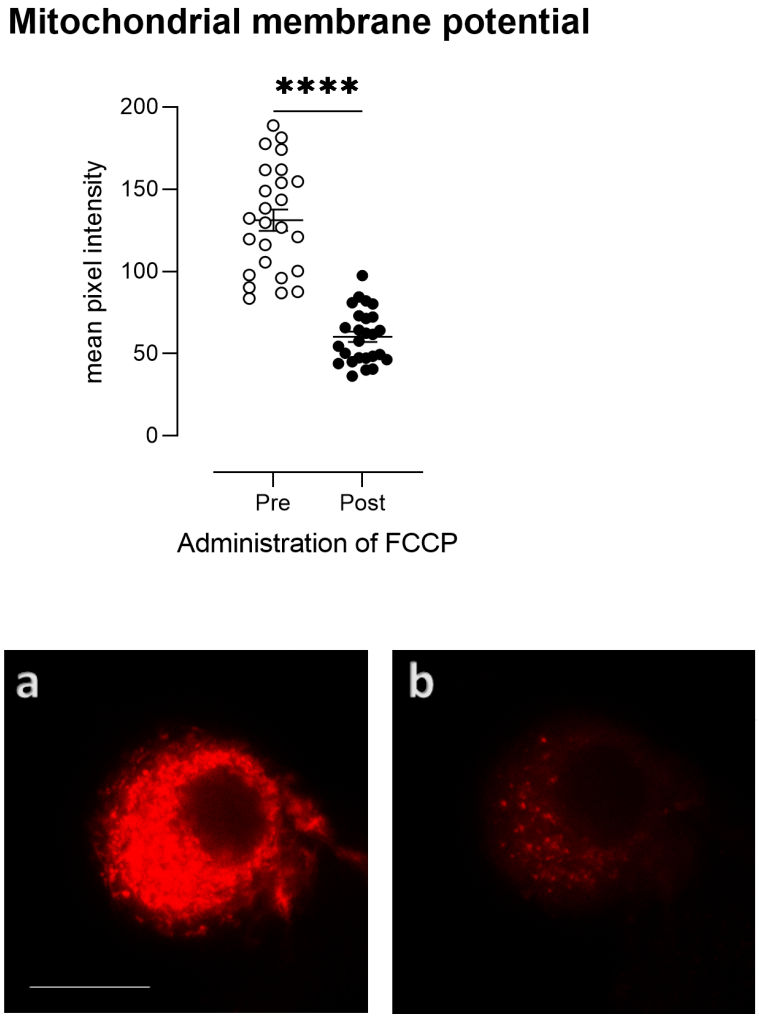

Fig. (19). Decrease in mitochondrial membrane potential caused by FCCP in hypoxia.

*Cells incubated in hypoxia were treated with 10 nM TMRM for 30 minutes. Baseline images of DRGs were obtained (a) and then cells were treated with 100 µM FCCP. Imaging took place between 4 and 23 minutes post treatment with FCCP. The pre-group represents cells with TMRM only and the post-group represents cells with TMRM + FCCP. Data were analysed using a Mann Whitney U test ****p < 0,0001. (a) DRG neurons treated with TMRM (b) DRG neurons treated with TMRM + FCCP. Scale bar = 250 µm*

3.2.4 Neuronal morphology with rotenone and L-DOPA

Since there was no significant change in mitochondrial membrane potential from the results obtained from the TMRM assay, we further examined the effect of rotenone and L-DOPA on neuronal morphology. Here, we studied the distribution and the morphology of neurons based upon beta-III tubulin immunofluorescence. Our results from multiple biological replicates did not show consistent evidence of cell death in neurons treated with rotenone, L-DOPA or both even at the highest concentrations used. Furthermore, we evaluated the effects of normoxia and hypoxia on the overall effects of rotenone and L-DOPA individually. Our result showed that L-DOPA does not have an effect on the neuronal morphology in both normoxia and hypoxia but some morphological changes were seen between normoxia and hypoxia with rotenone at 1 nM and 500 nM.

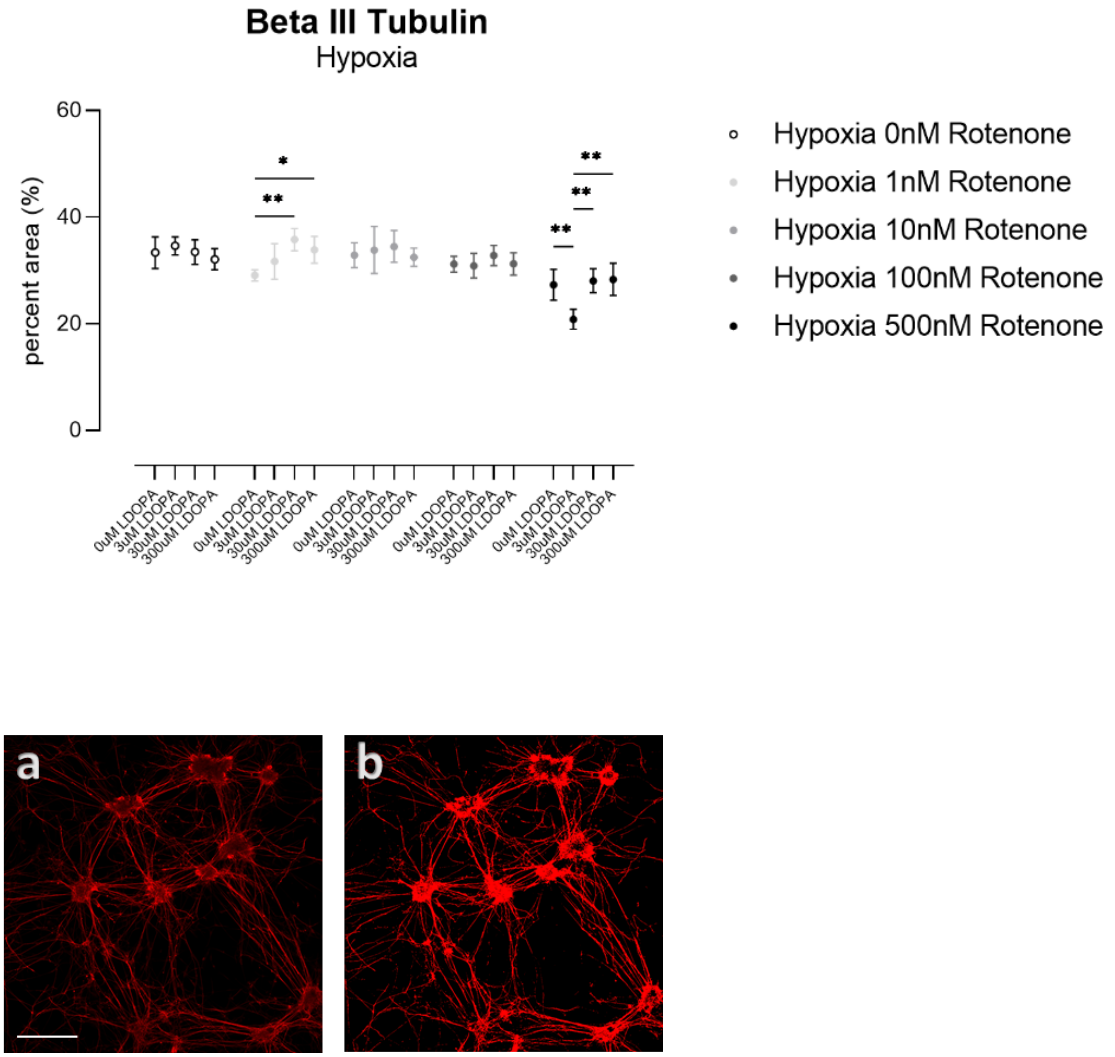

Fig. (20). No effect of rotenone or L-DOPA on DRG neuron morphology in hypoxia. *DRG neurons were treated with rotenone (1nM, 10nM, 100nM and 500nM) or DMSO as control and with 3μM, 30μM and 300μM L-DOPA or distilled water as control for L-DOPA. Effect of rotenone treatment F (4, 30) = 55,47; p < 0,0001. Effect of L-DOPA F (2,873, 86,19) = 6,775; p = 0,0005. Effect of rotenone + L-DOPA treatment F (12, 90) = 4,605; p < 0,0001. Tukey's multiple comparisons test was used to compare between and within different groups. No consistent reduction in beta III tubulin staining was observed. (a) Representative image of DRG neurons immunostained for beta III tubulin (b) Auto thresholded image on ImageJ. Scale bar = 100 μm.*

3.3 DISCUSSION

The preliminary study on the ideal concentration of rotenone in DRG cells indicated that concentrations between 1 - 500 nM are more suitable compared to 1μM. Nevertheless, several studies have used higher concentrations (Persson et al., 2013; Press & Milbrandt, 2008; Dedov et al., 2001). For example, Press & Milbrandt, 2008; treated DRG neurons with 2.5 μM rotenone for 72 hrs on the justification that there was a continued axonal degeneration post-treatment. However, it is noteworthy to mention that humans require several years of chronic exposure to rotenone in order to accelerate the risk of PD (Innos & Hickey, 2021). This implies that lower concentration given over a longer period of time might be much more translational than higher concentrations. Also, as rotenone solubility in typical vehicles such as DMSO and chloroform is about 50 mg/ml (Innos & Hickey, 2021), it is therefore highly unlikely that the concentration of rotenone at 1 μM and above will completely dissolve in DMSO.

In this study, our data showed oxidative stress by L-DOPA in DRG neurons was more consistent in normoxia at lower concentration of rotenone. There are two important points from this observation. First, the autoxidation of L-DOPA in normoxia could contribute to the increase in ROS production (Hörmann et al., 2021), thus explaining the increase in oxidative stress in normoxia. Unfortunately, most in-vitro studies on L-DOPA cytotoxicity have been performed in normoxia (Mena et al., 1992; Jin et al., 2010; Lai & Yu, 1997), implying that the results of these studies might have then been affected by the autoxidation problem (Hörmann et al., 2021). Second, low oxygen tension in the brain creates a hypoxic physiological environment in vivo compared to the level of oxygen in the atmosphere (Erecińska & Silver, 2001), therefore L-DOPA autoxidation in hypoxia is drastically reduced

as a result of more stability of L-DOPA. Thus, hypoxia limits this potential cytotoxin formation.

L-DOPA has been predicted, depending on its concentration, to have both neurotoxic and neuroprotective roles in previous in vitro studies (Zhong et al., 2014; Jami et al., 2014; Colamartino et al., 2012; Han et al., 2002). Our study did not show this dual action of L-DOPA, we clearly observed that low concentrations of L-DOPA (3 μM and 30 μM) in normoxia consistently causes oxidative stress although we did not record a similar trend in hypoxia. Zhong et al., 2014 reported that lower concentrations of L-DOPA (<30 μM) promote the proliferation and growth in PC12 cells treated with H_2O_2. However, neuronal cells do not respond similarly to L-DOPA-induced ROS compared to other human cell types, as they have limited glutathione-independent ability to scavenge ROS (Hörmann et al., 2021) but this glutathione-independent ROS defence mechanism has been shown to rely on utilisation of glutathione provided by astrocytes (Bolaños, 2016). Moreover, hypoxia induces expression of HIF1alpha in DRGs, which is neuroprotective against axonal injury (Cho et al., 2015).

Mitochondria plays a key role in the health of neuronal cells and impairment in mitochondria function has been linked to the pathology of PD and other neurodegenerative diseases (Betarbet et al., 2000; Franco-Iborra et al., 2015). Similarly, exposure to rotenone and other pesticides disrupt mitochondrial complex I thereby increasing the risk of PD (Innos & Hickey, 2021). However, overt reduction in mitochondrial membrane potential or of complex I activity is not required for accurate modelling of IPD in animals (Innos and Hickey. 2021). Our experiment explored the effect of rotenone and L-DOPA on mitochondrial membrane potential. SH-SY5Y cells treated with 100 nM rotenone were reported to show a reduction in TMRM fluorescence intensity indicating an impairment in mitochondrial function (Liang et

al., 2020). Some cells are more resistant to mitochondrial toxins. *Hipk2* $^{-/-}$ mouse brain tissues and mouse embryonic fibroblasts (MEFs) did not show any change in TMRM intensity upon treatment with (0.25, 0.5, 1, 2.5, or 5 nM) rotenone for 24 hours, an observation attributed to the elevation of parkin protein level (Zhang et al., 2019). DRG neurons, used in our study, are primary culture and may respond differently to rotenone compared to SH-SY5Y, an immortalised cell. In spite of the higher concentration (1nM, 10nM, 100nM and 500nM) of rotenone used, there was no significant reduction in the reduction in the fluorescence intensity and distribution of TMRM implying that the mitochondrial membranes were intact and thus the mitochondrial functions were not affected by rotenone. Indeed, a fraction of Hif1alpha, induced by hypoxia, is thought to translocate to mitochondria where it may reduce reactive species formation (Li et al., 2019).

Simiarly, there was no effect of L-DOPA on mitochondrial membrane potential using TMRM. Again, in a cell line (SH-SY5Y cells treated with 200 μM L-DOPA for 24 hours), a significant decrease in mitochondrial membrane potential using JC-10 dye has been observed (Giannopoulos et al., 2019). In this paper, the authors showed that mitochondrial function may be impaired when L-DOPA is miss-incorporated into microtubules in place of L-tyrosine, thereby affecting mitochondrial transport (Giannopoulos et al., 2019). The result from our FCCP assay further reinforces that the mitochondrial membrane in our treated DRG neurons were intact until they were decoupled upon treatment with FCCP. Although mitochondrial load in soma was normal (our TMRM data suggest this), it will be interesting to examine mitochondrial localisation in axons and our future experiments shall address this issue.

Finally, our results from the morphology of the neuron seeks to understand how rotenone and L-DOPA would affect neuronal morphology and whether they induced acute toxicity at

concentrations where oxidative stress was observed. Our data did not provide consistent and convincing evidence that L-DOPA resulted in significant loss of neurons or neurites in normoxia or hypoxia; however, future experiments shall examine later timepoints to further understand whether these agents interact to enhance their individual toxicities.

SUMMARY

Current data from the clinic suggest that L-DOPA may contribute to the development of PN in PD. Our results emphasise the importance of accurate modelling of the in vivo environment in in vitro experiments, in order to understand whether L-DOPA is a direct cause of PN in PD. Oxygen tension plays a key role in the toxicity of L-DOPA in vitro. Hypoxia, which is actually normoxia when compared with the in vivo environment, reduces the ability of rotenone and of L-DOPA to induce oxidative stress in vitro. In hypoxia, there is no additive effect of L-DOPA with rotenone, a toxin that increases the risk of development of PD in humans.

REFERENCES

Agamanolis, D. (2021, February). *Neuropathology*. Neuropathology. https://neuropathology-web.org/agamanolis.html

Ben Gedalya, T., Loeb, V., Israeli, E., Altschuler, Y., Selkoe, D. J., & Sharon, R. (2009). α-Synuclein and Polyunsaturated Fatty Acids Promote Clathrin-Mediated Endocytosis and Synaptic Vesicle Recycling. *Traffic*, *10*(2), 218–234. https://doi.org/10.1111/j.1600-0854.2008.00853.x

Berg, D., Postuma, R. B., Adler, C. H., Bloem, B. R., Chan, P., Dubois, B., Gasser, T., Goetz, C. G., Halliday, G., Joseph, L., Lang, A. E., Liepelt-Scarfone, I., Litvan, I., Marek, K., Obeso, J., Oertel, W., Olanow, C. W., Poewe, W., Stern, M., & Deuschl, G. (2015). MDS research criteria for prodromal Parkinson's disease. *Movement Disorders*, *30*(12), 1600–1611. https://doi.org/10.1002/mds.26431

Betarbet, R., Sherer, T. B., MacKenzie, G., Garcia-Osuna, M., Panov, A. V., & Greenamyre, J. T. (2000). Chronic systemic pesticide exposure reproduces features of Parkinson's disease. *Nature Neuroscience*, *3*(12), 1301–1306. https://doi.org/10.1038/81834

Bohnen, N. I., Muller, M. L. T. M., Kotagal, V., Koeppe, R. A., Kilbourn, M. A., Albin, R. L., & Frey, K. A. (2010). Olfactory dysfunction, central cholinergic integrity and cognitive impairment in Parkinson's disease. *Brain*, *133*(6), 1747–1754. https://doi.org/10.1093/brain/awq079

Bolaños, J. P. (2016). Bioenergetics and redox adaptations of astrocytes to neuronal activity. *Journal of Neurochemistry*, *139*(S2), 115–125. https://doi.org/10.1111/jnc.13486

Bratsos, S. P., Karponis, D., & Saleh, S. N. (2018). Efficacy and safety of deep brain stimulation in the treatment of parkinson's disease: A systematic review and meta-analysis of randomized controlled trials. *Cureus*. https://doi.org/10.7759/cureus.3474

Brundin, P., Dave, K. D., & Kordower, J. H. (2017). Therapeutic approaches to target alpha-synuclein pathology. *Experimental Neurology*, *298*, 225–235. https://doi.org/10.1016/j.expneurol.2017.10.003

Carreau, A., Hafny-Rahbi, B. E., Matejuk, A., Grillon, C., & Kieda, C. (2011). Why is the partial oxygen pressure of human tissues a crucial parameter? Small molecules and hypoxia. *Journal of Cellular and Molecular Medicine*, *15*(6), 1239–1253.

https://doi.org/10.1111/j.1582-4934.2011.01258.x

Casella, G. T. B., Wieser, R., Bunge, R. P., Margitich, I. S., Katz, J., Olson, L., & Wood, P. M. (2000). Density dependent regulation of human Schwann cell proliferation. *Glia*, *30*(2), 165–177. https://doi.org/10.1002/(sici)1098-1136(200004)30:2<165::aid-glia6>3.0.co;2-l

Ceravolo, R., Cossu, G., Bandettini di Poggio, M., Santoro, L., Barone, P., Zibetti, M., Frosini, D., Nicoletti, V., Manganelli, F., Iodice, R., Picillo, M., Merola, A., Lopiano, L., Paribello, A., Manca, D., Melis, M., Marchese, R., Borelli, P., Mereu, A., … Bonuccelli, U. (2013). Neuropathy and levodopa in Parkinson's disease: Evidence from a multicenter study. *Movement Disorders*, *28*(10), 1391–1397. https://doi.org/10.1002/mds.25585

Chernivec, E., Cooper, J., & Naylor, K. (2018). Exploring the Effect of Rotenone—A Known Inducer of Parkinson's Disease—On Mitochondrial Dynamics in Dictyostelium discoideum. *Cells*, *7*(11), 201. https://doi.org/10.3390/cells7110201

Chesselet, M.-F., & Richter, F. (2011). Modelling of Parkinson's disease in mice. *The Lancet Neurology*, *10*(12), 1108–1118. https://doi.org/10.1016/s1474-4422(11)70227-7

Cho, Y., Shin, J. E., Ewan, E. E., Oh, Y. M., Pita-Thomas, W., & Cavalli, V. (2015). Activating injury-responsive genes with hypoxia enhances axon regeneration through neuronal hif-1α. *Neuron*, *88*(4), 720–734. https://doi.org/10.1016/j.neuron.2015.09.050

Chung, K. K. K., Thomas, B., Li, X., Pletnikova, O., Troncoso, J. C., Marsh, L., Dawson, V. L., & Dawson, T. M. (2004). S -nitrosylation of parkin regulates ubiquitination and compromises parkin's protective function. *Science*, *304*(5675), 1328–1331. https://doi.org/10.1126/science.1093891

Colamartino, M., Padua, L., Meneghini, C., Leone, S., Cornetta, T., Testa, A., & Cozzi, R. (2012). Protective effects of l-dopa and carbidopa combined treatments on human catecholaminergic cells. *DNA and Cell Biology*, *31*(11), 1572–1579. https://doi.org/10.1089/dna.2011.1546

Conradt, C., Guo, D., Miclea, A., Nisslein, T., Ismail, C., Chatamra, K., & Andersohn, F. (2018). Increased Prevalence of Polyneuropathy in Parkinson's Disease Patients: An Observational Study. *Journal of Parkinson's Disease*, *8*(1), 141–144. https://doi.org/10.3233/jpd-161057

Cookson, M. R. (2015). LRRK2 pathways leading to neurodegeneration. *Current Neurology and Neuroscience Reports*, *15*(7). https://doi.org/10.1007/s11910-015-0564-y

Corti, O., Lesage, S., & Brice, A. (2011). What Genetics Tells us About the Causes and Mechanisms of Parkinson's Disease. *Physiological Reviews*, *91*(4), 1161–1218. https://doi.org/10.1152/physrev.00022.2010

Dedov, V. N., Mandadi, S., Armati, P. J., & Verkhratsky, A. (2001). Capsaicin-induced depolarisation of mitochondria in dorsal root ganglion neurons is enhanced by vanilloid receptors. *Neuroscience*, *103*(1), 219–226. https://doi.org/10.1016/s0306-4522(00)00540-6

Donadio, V., Incensi, A., Leta, V., Giannoccaro, M. P., Scaglione, C., Martinelli, P., Capellari, S., Avoni, P., Baruzzi, A., & Liguori, R. (2014). Skin nerve -synuclein deposits: A biomarker for idiopathic Parkinson disease. *Neurology*, *82*(15), 1362–1369. https://doi.org/10.1212/wnl.0000000000000316

Doppler, K., Weis, J., Karl, K., Ebert, S., Ebentheuer, J., Trenkwalder, C., Klebe, S., Volkmann, J., & Sommer, C. (2015). Distinctive distribution of phospho-alpha-synuclein in dermal nerves in multiple system atrophy. *Movement Disorders*, *30*(12), 1688–1692. https://doi.org/10.1002/mds.26293

Eisenhofer, G., Tian, H., Holmes, C., Matsunaga, J., Roffler-Tarlov, S., & Hearing, V. J. (2003). Tyrosinase: A developmentally specific major determinant of peripheral dopamine. *The FASEB Journal*, *17*(10), 1248–1255. https://doi.org/10.1096/fj.02-0736com

Emery, E. C., Luiz, A. P., Sikandar, S., Magnúsdóttir, R., Dong, X., & Wood, J. N. (2016). In vivo characterization of distinct modality-specific subsets of somatosensory neurons using GCaMP. *Science Advances*, *2*(11). https://doi.org/10.1126/sciadv.1600990

Erecińska, M., & Silver, I. A. (2001). Tissue oxygen tension and brain sensitivity to hypoxia. *Respiration Physiology*, *128*(3), 263–276. https://doi.org/10.1016/s0034-5687(01)00306-1

Fox, S. H., Katzenschlager, R., Lim, S.-Y., Barton, B., de Bie, R. M. A., Seppi, K., Coelho, M., & Sampaio, C. (2018). International Parkinson and movement disorder society evidence-based medicine review: Update on treatments for the motor symptoms of Parkinson's disease. *Movement Disorders*, *33*(8), 1248–1266. https://doi.org/10.1002/mds.27372

Franco-Iborra, S., Vila, M., & Perier, C. (2015). The parkinson disease mitochondrial hypothesis. *The Neuroscientist*, *22*(3), 266–277. https://doi.org/10.1177/1073858415574600

Geeven Gert. (2010). *Computational Statistics for the Identification of Transcriptional Gene*

Regulatory Networks.

Giannopoulos, S., Samardzic, K., Raymond, B. B. A., Djordjevic, S. P., & Rodgers, K. J. (2019). L-DOPA causes mitochondrial dysfunction in vitro: A novel mechanism of L-DOPA toxicity uncovered. *The International Journal of Biochemistry & Cell Biology*, *117*, 105624. https://doi.org/10.1016/j.biocel.2019.105624

Gispert, S., Ricciardi, F., Kurz, A., Azizov, M., Hoepken, H.-H., Becker, D., Voos, W., Leuner, K., Müller, W. E., Kudin, A. P., Kunz, W. S., Zimmermann, A., Roeper, J., Wenzel, D., Jendrach, M., García-Arencíbia, M., Fernández-Ruiz, J., Huber, L., Rohrer, H., … Auburger, G. (2009). Parkinson phenotype in aged pink1-deficient mice is accompanied by progressive mitochondrial dysfunction in absence of neurodegeneration. *PLoS ONE*, *4*(6), e5777. https://doi.org/10.1371/journal.pone.0005777

Goldberg, M. S., Pisani, A., Haburcak, M., Vortherms, T. A., Kitada, T., Costa, C., Tong, Y., Martella, G., Tscherter, A., Martins, A., Bernardi, G., Roth, B. L., Pothos, E. N., Calabresi, P., & Shen, J. (2005). Nigrostriatal dopaminergic deficits and hypokinesia caused by inactivation of the familial parkinsonism-linked gene DJ-1. *Neuron*, *45*(4), 489–496. https://doi.org/10.1016/j.neuron.2005.01.041

Han, S.-K., Mytilineou, C., & Cohen, G. (2002). l-DOPA Up-Regulates Glutathione and Protects Mesencephalic Cultures Against Oxidative Stress. *Journal of Neurochemistry*, *66*(2), 501–510. https://doi.org/10.1046/j.1471-4159.1996.66020501.x

Hancock, D. B., Martin, E. R., Mayhew, G. M., Stajich, J. M., Jewett, R., Stacy, M. A., Scott, B. L., Vance, J. M., & Scott, W. K. (2008). Pesticide exposure and risk of Parkinson's disease: A family-based case-control study. *BMC Neurology*, *8*(1). https://doi.org/10.1186/1471-2377-8-6

Healy, D. G., Falchi, M., O'Sullivan, S. S., Bonifati, V., Durr, A., Bressman, S., Brice, A., Aasly, J., Zabetian, C. P., Goldwurm, S., Ferreira, J. J., Tolosa, E., Kay, D. M., Klein, C., Williams, D. R., Marras, C., Lang, A. E., Wszolek, Z. K., Berciano, J., … Wood, N. W. (2008). Phenotype, genotype, and worldwide genetic penetrance of LRRK2-associated Parkinson's disease: A case-control study. *The Lancet Neurology*, *7*(7), 583–590. https://doi.org/10.1016/s1474-4422(08)70117-0

Hisahara, S., & Shimohama, S. (2011). Toxin-Induced and genetic animal models of parkinson's disease. *Parkinson's Disease*, *2011*, 1–14. https://doi.org/10.4061/2011/951709

Hlubocky, A., Wellik, K., Ross, M. A., Smith, B. E., Hoffman-Snyder, C., Demaerschalk, B. M., & Wingerchuk, D. M. (2010). Skin biopsy for diagnosis of small fiber neuropathy. *The Neurologist*, *16*(1), 61–63. https://doi.org/10.1097/nrl.0b013e3181c9c303

Hörmann, P., Delcambre, S., Hanke, J., Geffers, R., Leist, M., & Hiller, K. (2021). Impairment of neuronal mitochondrial function by l-DOPA in the absence of oxygen-dependent auto-oxidation and oxidative cell damage. *Cell Death Discovery*, *7*(1). https://doi.org/10.1038/s41420-021-00547-4

Ikebe, S., Tanaka, M., & Ozawa, T. (1995). Point mutations of mitochondrial genome in Parkinson's disease. *Molecular Brain Research*, *28*(2), 281–295. https://doi.org/10.1016/0169-328x(94)00209-w

Innos, J., & Hickey, M. A. (2021). Using rotenone to model parkinson's disease in mice: A review of the role of pharmacokinetics. *Chemical Research in Toxicology*, *34*(5), 1223–1239. https://doi.org/10.1021/acs.chemrestox.0c00522

Jami, M.-S., Pal, R., Hoedt, E., Neubert, T. A., Larsen, J. P., & Møller, S. G. (2014). Proteome analysis reveals roles of L-DOPA in response to oxidative stress in neurons. *BMC Neuroscience*, *15*(1). https://doi.org/10.1186/1471-2202-15-93

Jin, C. M., Yang, Y. J., Huang, H. S., Kai, M., & Lee, M. K. (2010). Mechanisms of L-DOPA-induced cytotoxicity in rat adrenal pheochromocytoma cells: Implication of oxidative stress-related kinases and cyclic AMP. *Neuroscience*, *170*(2), 390–398. https://doi.org/10.1016/j.neuroscience.2010.07.039

Kim, H.-J., Jeon, B. S., Lee, J.-Y., Cho, Y.-J., Hong, K.-S., & Cho, J.-Y. (2010). Taste function in patients with Parkinson disease. *Journal of Neurology*, *258*(6), 1076–1079. https://doi.org/10.1007/s00415-010-5884-x

Koprich, J. B., Johnston, T. H., Huot, P., Reyes, M. G., Espinosa, M., & Brotchie, J. M. (2011). Progressive neurodegeneration or endogenous compensation in an animal model of parkinson's disease produced by decreasing doses of alpha-synuclein. *PLoS ONE*, *6*(3), e17698. https://doi.org/10.1371/journal.pone.0017698

Krames, E. S. (2014). The role of the dorsal root ganglion in the development of neuropathic pain. *Pain Medicine*, *15*(10), 1669–1685. https://doi.org/10.1111/pme.12413

Lai, C.-T., & Yu, P. H. (1997). Dopamine- and l-β-3,4-dihydroxyphenylalanine hydrochloriDe (l-Dopa)-induced cytotoxicity towards catecholaminergic neuroblastoma SH-SY5Y Cells. *Biochemical Pharmacology*, *53*(3), 363–372. https://doi.org/10.1016/s0006-2952(96)00731-9

Li, H.-S., Zhou, Y.-N., Li, L., Li, S.-F., Long, D., Chen, X.-L., Zhang, J.-B., Feng, L., & Li, Y.-P. (2019). HIF-1α protects against oxidative stress by directly targeting mitochondria. *Redox Biology*, *25*, 101109. https://doi.org/10.1016/j.redox.2019.101109

Liang, T., Qian, Z.-M., Mu, M.-D., Yung, W.-H., & Ke, Y. (2020). Brain hepcidin suppresses major pathologies in experimental parkinsonism. *IScience*, *23*(7), 101284. https://doi.org/10.1016/j.isci.2020.101284

Liu, C.-N., Wall, P. D., Ben-Dor, E., Michaelis, M., Amir, R., & Devor, M. (2000). Tactile allodynia in the absence of C-fiber activation: Altered firing properties of DRG neurons following spinal nerve injury. *Pain*, *85*(3), 503–521. https://doi.org/10.1016/s0304-3959(00)00251-7

Mancini, F., Comi, C., Oggioni, G. D., Pacchetti, C., Calandrella, D., Coletti Moja, M., Riboldazzi, G., Tunesi, S., Dal Fante, M., Manfredi, L., Lacerenza, M., Cantello, R., & Antonini, A. (2014). Prevalence and features of peripheral neuropathy in Parkinson's disease patients under different therapeutic regimens. *Parkinsonism & Related Disorders*, *20*(1), 27–31. https://doi.org/10.1016/j.parkreldis.2013.09.007

Marquez-Infante, C., Murphy, S. M., Mathew, L., Alsanousi, A., Lunn, M. P., Brandner, S., Yousry, T. A., Blake, J., & Reilly, M. M. (2013). Asymmetric sensory ganglionopathy: A case series. *Muscle & Nerve*, *48*(1), 145–150. https://doi.org/10.1002/mus.23772

Meiser, J., Weindl, D., & Hiller, K. (2013). Complexity of dopamine metabolism. *Cell Communication and Signaling*, *11*(1). https://doi.org/10.1186/1478-811x-11-34

Mena, M. A., Pardo, B., Casarejos, M. J., Fahn, S., & de Yébenes, J. G. (1992). Neurotoxicity of levodopa on catecholamine-rich neurons. *Movement Disorders*, *7*(1), 23–31. https://doi.org/10.1002/mds.870070105

Misra, U., Kalita, J., & Nair, P. (2008). Diagnostic approach to peripheral neuropathy. *Annals of Indian Academy of Neurology*, *11*(2), 89. https://doi.org/10.4103/0972-2327.41875

Müller, T., Laar, T. van, Cornblath, D. R., Odin, P., Klostermann, F., Grandas, F. J., Ebersbach, G., Urban, P. P., Valldeoriola, F., & Antonini, A. (2013). Peripheral neuropathy in Parkinson's disease: Levodopa exposure and implications for duodenal delivery. *Parkinsonism & Related Disorders*, *19*(5), 501–507. https://doi.org/10.1016/j.parkreldis.2013.02.006

Nolano, M., Provitera, V., Estraneo, A., Selim, M. M., Caporaso, G., Stancanelli, A., Saltalamacchia, A. M., Lanzillo, B., & Santoro, L. (2008). Sensory deficit in

Parkinson's disease: Evidence of a cutaneous denervation. *Brain*, *131*(7), 1903–1911. https://doi.org/10.1093/brain/awn102

Okyere, S. K., Zeng, C., Yue, D., & Hu, Y. (2021). Neurotoxic mechanism and shortcomings of MPTP, 6-OHDA, rotenone and paraquat-induced parkinson's disease animal models. *Venoms and Toxins*, *1*(1), 27–40. https://doi.org/10.2174/2666121701999201104163407

Ortuño-Lizarán, I., Beach, T. G., Serrano, G. E., Walker, D. G., Adler, C. H., & Cuenca, N. (2018). Phosphorylated α-synuclein in the retina is a biomarker of Parkinson's disease pathology severity. *Movement Disorders*, *33*(8), 1315–1324. https://doi.org/10.1002/mds.27392

Parmar, M., Grealish, S., & Henchcliffe, C. (2020). The future of stem cell therapies for Parkinson disease. *Nature Reviews Neuroscience*, *21*(2), 103–115. https://doi.org/10.1038/s41583-019-0257-7

Persson, A.-K., Kim, I., Zhao, P., Estacion, M., Black, J. A., & Waxman, S. G. (2013). Sodium channels contribute to degeneration of dorsal root ganglion neurites induced by mitochondrial dysfunction in an in vitro model of axonal injury. *Journal of Neuroscience*, *33*(49), 19250–19261. https://doi.org/10.1523/jneurosci.2148-13.2013

Picconi, B., Hernández, L. F., Obeso, J. A., & Calabresi, P. (2017). Motor complications in Parkinson's disease: Striatal molecular and electrophysiological mechanisms of dyskinesias. *Movement Disorders*, *33*(6), 867–876. https://doi.org/10.1002/mds.27261

Planken, A., Kurvits, L., Reimann, E., Kadastik-Eerme, L., Kingo, K., Kõks, S., & Taba, P. (2017). Looking beyond the brain to improve the pathogenic understanding of Parkinson's disease: Implications of whole transcriptome profiling of Patients' skin. *BMC Neurology*, *17*(1). https://doi.org/10.1186/s12883-016-0784-z

Platika, D., Boulos, M. H., Baizer, L., & Fishman, M. C. (1985). Neuronal traits of clonal cell lines derived by fusion of dorsal root ganglia neurons with neuroblastoma cells. *Proceedings of the National Academy of Sciences*, *82*(10), 3499–3503. https://doi.org/10.1073/pnas.82.10.3499

Podgorny, P. J., Suchowersky, O., Romanchuk, K. G., & Feasby, T. E. (2016). Evidence for small fiber neuropathy in early Parkinson's disease. *Parkinsonism & Related Disorders*, *28*, 94–99. https://doi.org/10.1016/j.parkreldis.2016.04.033

Poewe, W., Seppi, K., Tanner, C. M., Halliday, G. M., Brundin, P., Volkmann, J., Schrag, A.-E., & Lang, A. E. (2017). Parkinson disease. *Nature Reviews Disease Primers*, *3*(1). https://doi.org/10.1038/nrdp.2017.13

Polymeropoulos, M. H. (1998). Autosomal dominant Parkinson's disease. *Journal of Neurology*, *245*(S3), P1–P3. https://doi.org/10.1007/pl00007740

Polymeropoulos, M. H., Lavedan, C., Leroy, E., Ide, S. E., Dehejia, A., Dutra, A., Pike, B., Root, H., Rubenstein, J., Boyer, R., Stenroos, E. S., Chandrasekharappa, S., Athanassiadou, A., Papapetropoulos, T., Johnson, W. G., Lazzarini, A. M., Duvoisin, R. C., Di Iorio, G., Golbe, L. I., & Nussbaum, R. L. (1997). Mutation in the α-Synuclein Gene Identified in Families with Parkinson's Disease. *Science*, *276*(5321), 2045–2047. https://doi.org/10.1126/science.276.5321.2045

Pont-Sunyer, C., Hotter, A., Gaig, C., Seppi, K., Compta, Y., Katzenschlager, R., Mas, N., Hofeneder, D., Brücke, T., Bayés, A., Wenzel, K., Infante, J., Zach, H., Pirker, W., Posada, I. J., Álvarez, R., Ispierto, L., De Fàbregues, O., Callén, A., … Tolosa, E. (2014). The Onset of Nonmotor Symptoms in Parkinson's disease (The ONSET PDStudy). *Movement Disorders*, *30*(2), 229–237. https://doi.org/10.1002/mds.26077

Press, C., & Milbrandt, J. (2008). Nmnat delays axonal degeneration caused by mitochondrial and oxidative stress. *Journal of Neuroscience*, *28*(19), 4861–4871. https://doi.org/10.1523/jneurosci.0525-08.2008

Ren, X., Zou, Q., Yuan, C., Chang, R., Xing, R., & Yan, X. (2019). The dominant role of oxygen in modulating the chemical evolution pathways of tyrosine in peptides: Dityrosine or melanin. *Angewandte Chemie International Edition*, *58*(18), 5872–5876. https://doi.org/10.1002/anie.201814575

Romagnolo, A., Merola, A., Artusi, C. A., Rizzone, M. G., Zibetti, M., & Lopiano, L. (2018). Levodopa‐Induced neuropathy: A systematic review. *Movement Disorders Clinical Practice*, *6*(2), 96–103. https://doi.org/10.1002/mdc3.12688

Sardi, S. P., Cedarbaum, J. M., & Brundin, P. (2018). Targeted therapies for parkinson's disease: From genetics to the clinic. *Movement Disorders*, *33*(5), 684–696. https://doi.org/10.1002/mds.27414

Shahrizaila, N., Mahamad, U. A., Yap, A.-C., Choo, Y.-M., Marras, C., & Lim, S.-Y. (2013). Is chronic levodopa therapy associated with distal symmetric polyneuropathy in Parkinson's disease? *Parkinsonism & Related Disorders*, *19*(3), 391–393. https://doi.org/10.1016/j.parkreldis.2012.08.002

Shihabuddin, L. S., Brundin, P., Greenamyre, J. T., Stephenson, D., & Sardi, S. P. (2018). New frontiers in parkinson's disease: From genetics to the clinic. *The Journal of Neuroscience*, *38*(44), 9375–9382. https://doi.org/10.1523/jneurosci.1666-18.2018

Shulman, L. M., Gruber-Baldini, A. L., Anderson, K. E., Fishman, P. S., Reich, S. G., &

Weiner, W. J. (2010). The clinically important difference on the unified parkinson's disease rating scale. *Archives of Neurology*, *67*(1). https://doi.org/10.1001/archneurol.2009.295

Simon, C. (2009). Peripheral neuropathy. *InnovAiT: Education and Inspiration for General Practice*, *2*(9), 538–545. https://doi.org/10.1093/innovait/inp129

Sun, L., Jiang, W.-W., Wang, Y., Yuan, Y.-S., Rong, Z., Wu, J., Fan, Y., Lu, M., & Zhang, K.-Z. (2021). Phosphorylated α-synuclein aggregated in Schwann cells exacerbates peripheral neuroinflammation and nerve dysfunction in Parkinson's disease through TLR2/NF-κB pathway. *Cell Death Discovery*, *7*(1). https://doi.org/10.1038/s41420-021-00676-w

Tanner, C. M., Kamel, F., Ross, G. W., Hoppin, J. A., Goldman, S. M., Korell, M., Marras, C., Bhudhikanok, G. S., Kasten, M., Chade, A. R., Comyns, K., Richards, M. B., Meng, C., Priestley, B., Fernandez, H. H., Cambi, F., Umbach, D. M., Blair, A., Sandler, D. P., & Langston, J. W. (2011). Rotenone, Paraquat, and parkinson's disease. *Environmental Health Perspectives*, *119*(6), 866–872. https://doi.org/10.1289/ehp.1002839

Themistocleous, A. C., Ramirez, J. D., Serra, J., & Bennett, D. L. H. (2014). The clinical approach to small fibre neuropathy and painful channelopathy. *Practical Neurology*, *14*(6), 368–379. https://doi.org/10.1136/practneurol-2013-000758

Tieu, K. (2011). A guide to neurotoxic animal models of parkinson's disease. *Cold Spring Harbor Perspectives in Medicine*, *1*(1), a009316–a009316. https://doi.org/10.1101/cshperspect.a009316

Vacchi, E., Senese, C., Chiaro, G., Disanto, G., Pinton, S., Morandi, S., Bertaina, I., Bianco, G., Staedler, C., Galati, S., Gobbi, C., Kaelin-Lang, A., & Melli, G. (2021). Alpha-synuclein oligomers and small nerve fiber pathology in skin are potential biomarkers of Parkinson's disease. *Npj Parkinson's Disease*, *7*(1). https://doi.org/10.1038/s41531-021-00262-y

Valek, L., Tran, B., Wilken‐Schmitz, A., Trautmann, S., Heidler, J., Schmid, T., Brüne, B., Thomas, D., Deller, T., Geisslinger, G., Auburger, G., & Tegeder, I. (2021). Prodromal sensory neuropathy in Pink1 −/− SNCA A53T double mutant Parkinson mice. *Neuropathology and Applied Neurobiology*, *47*(7), 1060–1079. https://doi.org/10.1111/nan.12734

Vivacqua, G., Yin, J.-J., Casini, A., Li, X., Li, Y.-H., D'Este, L., Chan, P., Renda, T. G., & Yu, S. (2009). Immunolocalization of alpha-synuclein in the rat spinal cord by two

novel monoclonal antibodies. *Neuroscience*, *158*(4), 1478–1487. https://doi.org/10.1016/j.neuroscience.2008.12.001

Wang, N., Gibbons, C. H., Lafo, J., & Freeman, R. (2013). -Synuclein in cutaneous autonomic nerves. *Neurology*, *81*(18), 1604–1610. https://doi.org/10.1212/wnl.0b013e3182a9f449

Zambito Marsala, S., Tinazzi, M., Vitaliani, R., Recchia, S., Fabris, F., Marchini, C., Fiaschi, A., Moretto, G., Giometto, B., Macerollo, A., & Defazio, G. (2010). Spontaneous pain, pain threshold, and pain tolerance in Parkinson's disease. *Journal of Neurology*, *258*(4), 627–633. https://doi.org/10.1007/s00415-010-5812-0

Zeuner, K. E., Schäffer, E., Hopfner, F., Brüggemann, N., & Berg, D. (2019). Progress of pharmacological approaches in parkinson's disease. *Clinical Pharmacology & Therapeutics*, *105*(5), 1106–1120. https://doi.org/10.1002/cpt.1374

Zhang, J., Shang, Y., Kamiya, S., Kotowski, S. J., Nakamura, K., & Huang, E. J. (2019). Loss of HIPK2 protects neurons from mitochondrial toxins by regulating parkin protein turnover. *The Journal of Neuroscience*, *40*(3), 557–568. https://doi.org/10.1523/jneurosci.2017-19.2019

Zhong, S.-Y., Chen, Y.-X., Fang, M., Zhu, X.-L., Zhao, Y.-X., & Liu, X.-Y. (2014). Low-Dose Levodopa Protects Nerve Cells from Oxidative Stress and Up-Regulates Expression of pCREB and CD39. *PLoS ONE*, *9*(4), e95387. https://doi.org/10.1371/journal.pone.0095387

Zis, P., Grünewald, R. A., Chaudhuri, R. K., & Hadjivassiliou, M. (2017). Peripheral neuropathy in idiopathic Parkinson's disease: A systematic review. *Journal of the Neurological Sciences*, *378*, 204–209. https://doi.org/10.1016/j.jns.2017.05.023

ACKNOWLEDGEMENT

I am most grateful for the opportunity to carry out my thesis under the supervision of **Dr. Miriam A. Hickey**. She is a teacher and mentor indeed. The last one year has been very interesting doing science. I also acknowledge every member of the Laboratory of Neurodegenerative Disease Therapeutics (Hickey Lab) particularly, **Dr. Maili Jacobson** for her encouragement all the way and **Ulla Peterson** for helping with DRG cell culture.

NON-EXCLUSIVE LICENCE TO REPRODUCE THE THESIS AND MAKE THE THESIS PUBLIC

I, Oyedele J. OLAOYE

1. grant the University of Tartu a free permit (non-exclusive licence) to:

reproduce, for the purpose of preservation, including for adding to the DSpace digital archives until the expiry of the term of copyright, my thesis

Investigation of Dopamine-mediated Toxicity in Parkinsonian Sensory Neurons

supervised by **Dr. Miriam A. HICKEY**,

2. I grant the University of Tartu the permit to make the thesis specified in point 1 available to the public via the web environment of the University of Tartu, including via the DSpace digital archives, under the Creative Commons licence CC BY NC ND 4.0, which allows, by giving appropriate credit to the author, to reproduce, distribute the work and communicate it to the public, and prohibits the creation of derivative works and any commercial use of the work from ***27/05/2022*** until the expiry of the term of copyright,

3. I am aware that the author retains the rights specified in points 1 and 2.

4. I confirm that granting the non-exclusive licence does not infringe other persons' intellectual property rights or rights arising from the personal data protection legislation.

Oyedele J. OLAOYE

27/05/2022

To the vice dean for academic affairs of the Faculty of _____, University of Tartu

Application for establishing restrictions on the publishing of the graduation thesis, and declaring the defence private

Name _____
Date of birth _____
Curriculum _____
Supervisor _____
Graduation thesis title _____
_____

[X] I request my graduation thesis not to be published until …26.05.2025……(date) for the reason indicated below:

- [ ] Economic copyright rights belong to other people
- [ ] Thesis includes personal data and the data subject has not agreed to publishing
- [ ] State secret
- [ ] Trade secret
- [X] In future, the graduation thesis will be published as a scientific article
- [ ] Other reasons

Explanation (reasons why restrictions are applied for and why for the particular period):

We request that this thesis not be published as this would jeopardise our ability to publish findings in an academic journal.

[ ] I request my defence to be declared private.
Explanation (reasons for declaring the defence private):

Application has the following annexes (to be filled in if there are annexes, i.e. the company's confirmation that the thesis involves a trade secret):

1. Thesis
2.

Date and student's signature _____

Date and supervisor's signature _____